

ACCEPTED MANUSCRIPT

Peptide-based assembled nanostructures that can direct cellular responses

To cite this article before publication: Haofu Huang *et al* 2022 *Biomed. Mater.* in press <https://doi.org/10.1088/1748-605X/ac92b5>

Manuscript version: Accepted Manuscript

Accepted Manuscript is “the version of the article accepted for publication including all changes made as a result of the peer review process, and which may also include the addition to the article by IOP Publishing of a header, an article ID, a cover sheet and/or an ‘Accepted Manuscript’ watermark, but excluding any other editing, typesetting or other changes made by IOP Publishing and/or its licensors”

This Accepted Manuscript is © 2022 IOP Publishing Ltd.

During the embargo period (the 12 month period from the publication of the Version of Record of this article), the Accepted Manuscript is fully protected by copyright and cannot be reused or reposted elsewhere.

As the Version of Record of this article is going to be / has been published on a subscription basis, this Accepted Manuscript is available for reuse under a CC BY-NC-ND 3.0 licence after the 12 month embargo period.

After the embargo period, everyone is permitted to use copy and redistribute this article for non-commercial purposes only, provided that they adhere to all the terms of the licence <https://creativecommons.org/licenses/by-nc-nd/3.0>

Although reasonable endeavours have been taken to obtain all necessary permissions from third parties to include their copyrighted content within this article, their full citation and copyright line may not be present in this Accepted Manuscript version. Before using any content from this article, please refer to the Version of Record on IOPscience once published for full citation and copyright details, as permissions will likely be required. All third party content is fully copyright protected, unless specifically stated otherwise in the figure caption in the Version of Record.

View the [article online](#) for updates and enhancements.

Peptide-based assembled nanostructures that can direct cellular responses

Haofu Huang¹, Kristi Kiick^{1,2,3}

¹ Department of Materials Science and Engineering, University of Delaware, Newark, DE, 19716, USA

² Department of Biomedical Engineering, University of Delaware, Newark, DE, 19716, USA

³ Delaware Biotechnology Institute, Newark, DE, 19711, USA

E-mail: huanghf@udel.edu and kiick@udel.edu

Received xxxxxx

Accepted for publication xxxxxx

Published xxxxxx

Abstract

Natural originated materials have been well-studied over the past several decades owing to their higher biocompatibility compared to the traditional polymers. Peptides, consisting of amino acids, are among the most popular programable building blocks, which is becoming a growing interest in nanobiotechnology. Structures assembled using those biomimetic peptides allow the exploration of chemical sequences beyond those been routinely used in biology. In this Review, we discussed the most recent experimental discoveries on the peptide-based assembled nanostructures and their potential application at the cellular level such as drug delivery. In particular, we explored the fundamental principles of peptide self-assembly and the most recent development in improving their interactions with biological systems. We believe that as the fundamental knowledge of the peptide assemblies evolves, the more sophisticated and versatile nanostructures can be built, with promising biomedical applications.

Keywords: Peptides; Self-assembly; Nanoparticles; Secondary structures; Bioactive materials; Drug delivery; Stimuli-responsiveness; Cellular uptake; Anti-tumor drug target

1. Introduction

Self-assembly is the process by which unordered materials are arranged into highly organized structures without the need to apply external forces¹. Living cells and tissues contain a variety of self-assembled structures that contribute to mechanical support and biochemical function. For example, self-assembled collagen fibers, the most abundant component in the extracellular matrix (ECM), play an essential role in the load-bearing capacity of musculoskeletal tissues as well as in cell adhesion and growth²⁻⁴. The DNA double helix⁵ and bilayer membranes from lipids^{6,7}, are also self-assembled structures that encode/protect genetic information and compartmentalize macromolecules. Inspired by these naturally occurring and highly functional self-assembled components of living systems, biomolecular self-assembly has remained an area of

intense scientific investigation in the production of nano- and micro-scale materials with a variety of shapes⁸⁻¹² and novel functional properties^{11,13-16}.

Self-assembly is directed by the physicochemical properties of the assembling motifs and the local interactions within and between them. Hydrogen bonding, π - π stacking interactions, hydrophobic interaction, electrostatic interactions, and van der Waals forces combined to help assembled structures maintain a stable, minimal energy state^{1,17}. For example, in the formation of a DNA double helix, two nucleic acids are bound to each other by the hydrogen bond¹⁸. Whereas in the formation of proteins, the combination of those interactions rearranges the spatial positioning of different amino acids, resulting in the formation of a variety of secondary structures such as α -helix, β -sheet, and polyproline helix, among many others¹⁹. Taking these self-assembling building blocks as models, biomolecules such as lipids, peptides, or nucleic acids have been widely used as

building blocks to create novel and sophisticated nanomaterials, such as programmed 2-dimensional self-assemblies of DNA²⁰⁻²², antimicrobial peptides^{23,24}, peptide- and DNA-based biocatalysts²⁵⁻²⁷, and molecular probes for bioimaging^{28,29}.

Nanoparticles (NPs) are a subcategory of nanomaterials that are at the forefront of contemporary nanotechnology research and development, with a compound annual growth rate (CAGR) of 16% [Global Nanoparticle Market Outlook 2020] and anticipated a 36.4% CAGR from 2021 to 2030 [Nanotechnology Market Outlook – 2030]. In general, NPs are particles with diameters that range between 1 nm to 100 nm³⁰; because of their small size, NPs are able to penetrate tissues, as well as enter cells^{31,32}. With certain modifications (such as functionalization with poly(ethylene glycol) (PEG)), NPs can be engineered with increased residence time in vivo, due to a reduction in their opsonization³³. Furthermore, attributed to relatively high solubility, NPs possess enhanced bioavailability compared to free hydrophobic drugs³⁴⁻³⁷, so the encapsulation of drugs in appropriate nanoparticles significantly improves drug dosing efficiency. However, penetration of NPs into cell membranes can remain a key barrier, and methods to improve cellular uptake such as targeting select cells, and activating specific uptake and membrane penetration mechanisms, remain an area of active investigation.

Polymeric NPs have attracted considerable interest over recent years due to their properties resulting from their small size^{38,39}, stimuli-responsiveness^{40,41}, and improved cytocompatibility^{42,43}. Amphiphilic polymeric NPs, which contain a hydrophilic head and a hydrophobic tail, have been widely used as drug carriers owing to the potential controlled release of drugs and the ability to protect the drugs against the environment³⁸. Some novel studies have been conducted to wrap the nucleic-acid-encapsulated polymeric NPs with cancer cell membranes⁴⁴⁻⁴⁷ and human megakaryocyte membranes⁴⁸⁻⁵⁰. The membrane-coated exterior of these NPs grants high bioavailability^{44-46,49-52}, cell-targeting ability^{49,50}, and can also be used in photothermal therapy^{46,51}. However, challenges still remain, such as the toxicity at high polymer concentration⁵³ and the biodegradation of polymeric NPs⁵⁴.

Liposomes are spherical vesicles comprising a bilayer of amphiphilic phospholipids⁵⁵, which share a close resemblance to the composition of mammalian cell membranes, enabling efficient interactions between the membrane and the lipid bilayers thus improving cellular uptake⁵⁶. Nevertheless, many liposomes are recognized as foreign by the reticuloendothelial system, thus resulting in rapid removal from circulation⁵⁷, and liposomes can also exhibit short shelf lives owing to the instability of the lipid bilayers⁵⁷. New classes of NPs have emerged to address some of these limitations of liposomes or other polymeric NPs.

Because of their chemical and biochemical versatility and relative stability, amphiphilic peptides, which comprise a hydrophobic tail (either aliphatic or peptide in origin) and a hydrophilic 'head', have garnered steady attention in the nanomaterials field. Their assembly is driven largely by hydrophobic interactions and hydrogen bonding, which support the self-assembly of different nanostructures for utilization as therapeutic agents to treat diseases by transporting drugs across membranes to specific sites. These materials have specific benefits: 1) Peptides are easily synthesized and scaled up using solid-phase peptide synthesis or recombinant DNA technology^{58,59}. 2) Attributed to their natural origin, peptide NPs can exhibit relatively high biocompatibility and bioavailability^{24,60,61}. 3) More than 20 types of naturally occurring amino acids provide a large variety of functional groups, including but not limited to thiols, carboxylic acids, amines, and the ability to incorporate myriad non-natural chemical functionalities, such as azides, alkynes, and tetrazines (among others) further expands this versatility and bio-orthogonality. 4) The naturally formed secondary structures such as the α -helix or β -sheet can induce bottom-up construction of nanostructures such as spheres, cylinders, tubes, and other novel morphologies that can occur via self-assembly in an aqueous solution⁶². With the ability to expand their functionality by conjugating peptide-based NPs with other molecules such as fatty acids or polysaccharides⁶³⁻⁶⁵, they can be utilized as biocatalysts⁶⁵ or drug delivery carriers⁶⁴. Gene delivery is also a more recent, but commonly reported application of peptide NPs⁶⁶⁻⁶⁸.

Small-molecule drugs have been a pillar of the modern pharmaceutical industry⁶⁹, but as mentioned above, have challenges regarding bioavailability and high necessary dosing frequencies that can cause undesired side effects such as liver and kidney damage^{70,71}. Peptide-based NPs can encapsulate hydrophobic drugs within their hydrophobic domain through hydrophobic interaction⁷²⁻⁷⁴ to prevent uncontrolled precipitation at the injection site and retain solubility with the help of the hydrophilic domain. Without exposure to the hydrophilic environment, the transfer of hydrophobic drugs through cell membranes can be enhanced by NPs. By tuning the physical or chemical properties of the NPs, the sustained release of drugs has been well developed^{75,76}, resulting in a longer release time and lower dosing frequency, thus decreasing the cytotoxicity caused by uncontrolled drug release. Furthermore, peptides with target-binding abilities have been developed to overcome the rapid removal of NPs by physiological fluid^{28,76-78} for a longer release window.

We are particularly interested in the molecular design of self-assembled peptide-based NPs for advanced drug delivery and corresponding modification of cellular responses. In this article, we focus on recent studies of self-assembled peptides and their advanced application, highlighting the adaptability

of peptide-based NPs owing to the high level of specificity in their design and chemical functionality. Moreover, it is convenient to engineer multiple functions in a single assembled structure, which can promote the performance of the whole system with a synergistic effect. Other recent studies regarding polymeric NPs^{38,79–81}, metallic NPs^{82–84}, and inorganic NPs^{85–87} have been well summarized in other published reviews.

2. Self-assembled peptide building blocks

2.1 α -helical and coiled-coil peptides

The most common secondary structure found in globular proteins is the α -helix. For decades, the α -helix has been well studied for its properties and recognized for its promotion of signaling pathways, molecular transport, and hierarchical structures in cells⁸⁸. It has more recently been applied as a key component in building novel biomaterials^{89–93}. Novel design of fibrillar, tubes, and sphere nanostructures⁹² has been enabled by the right-hand helical conformation of the α -helical synthetic peptides, stabilized by hydrogen bonding between backbone amide and carbonyl groups⁹⁴. For example, filamentous nanostructures can be generated from coiled-coil peptide motifs 25–50 residues long^{91,95}, and unilamellar spherical cages with diameters of ~ 100 nm have also been generated^{92,96}. Recently studies showed a growing trend to utilize the coiled-coil structure, which is constructed by the α -helix, as a building block for building peptide nanostructures^{97–100}.

The coiled-coil is a structural motif in proteins in which 2–7 α -helices are coiled together similar to the strands of a rope¹⁰¹. These peptides were based on heptad repeats (abcdefg)_n, with positions a and d being occupied by hydrophobic residues and polar residues anywhere else in the sequence. Hydrophobic residues form an inter-helical

hydrophobic core, providing a stabilizing interface between the helices, while charged residues at positions e and g participate in electrostatic interactions contributing to coiled-coil stability. These peptides form 2–5 helices that wrap around each other in a super-helical fashion to form nanoscale fibers. Most studies have focused on making fibrillar coiled-coil structures, although some recent studies have demonstrated alternative ways to utilize the coiled-coil motif for forming other types of structures, such as sphere morphology^{102,103} and cross-linked hydrogels for therapeutic applications^{97,104}.

Barns *et al.* successfully synthesized triblock copolypeptides based on coiled-coil structures¹⁰⁵, which can self-assemble into nanovesicles with the help of the leucine zipper (Figure 1A). In their work, instead of using traditional solid-phase peptide synthesis (SPPS), a convenient ring-opening polymerization (ROP) was employed to synthesize the poly (leucine-valine) peptide with the sequence PEO₁₁₃-PLV₆-PK₃₀. In contrast to traditional coiled coils, the peptide design employed all hydrophobic residues (leucine and valine) on the (abcdefg) heptad repeats, but still formed a stable structure with a circular dichroism spectrum similar to that of a coiled-coil in aqueous solution (Figure 1B). The self-assembly of the vesicle-like structure was induced by slowly pouring acidic (pH 2), leucine-insoluble buffer into a poly(ethylene oxide)-rich trifluoroacetic acid (TFA) solution, via a solvent-exchange technique. The average diameter of the assembled vesicles was 94 nm (confirmed via transmission electron microscopy (TEM) measurements (Figure 1A)). By analyzing the hydrophobic percentage of the polymer (only 6 wt%), the authors concluded that the leucine-rich domain dominates the thermodynamics of self-assembly by defining a low interfacial curvature of the assembly, resulting in vesicle morphologies. Furthermore, the sizes of the vesicles can be tuned by modifying the amount of buffer used in the solvent

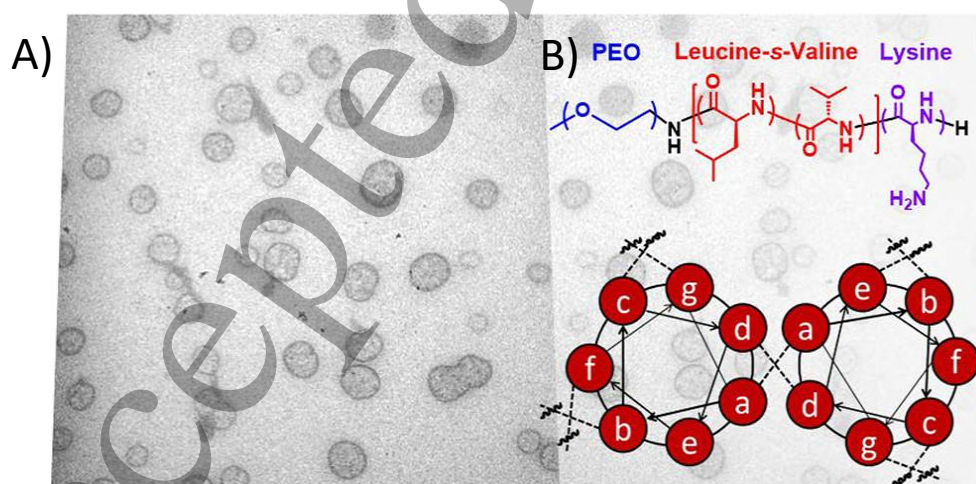


Figure 1 Defined structures of the PEO₁₁₃-PLV₆-PK₃₀ molecule. A) TEM micrograph shows the vesicle-like structure with radius around 100 nm; B) Proposed interaction pattern in a homopoly(leucine) block polymer in Barns' work; Reprinted with permission¹⁰⁵. Copyright 2020, American Chemical Society.

switch, which broadens the possibility for fabricating vesicles for alternative usage¹⁰². hydrogen bonding to stabilize the β -sheet, which improves

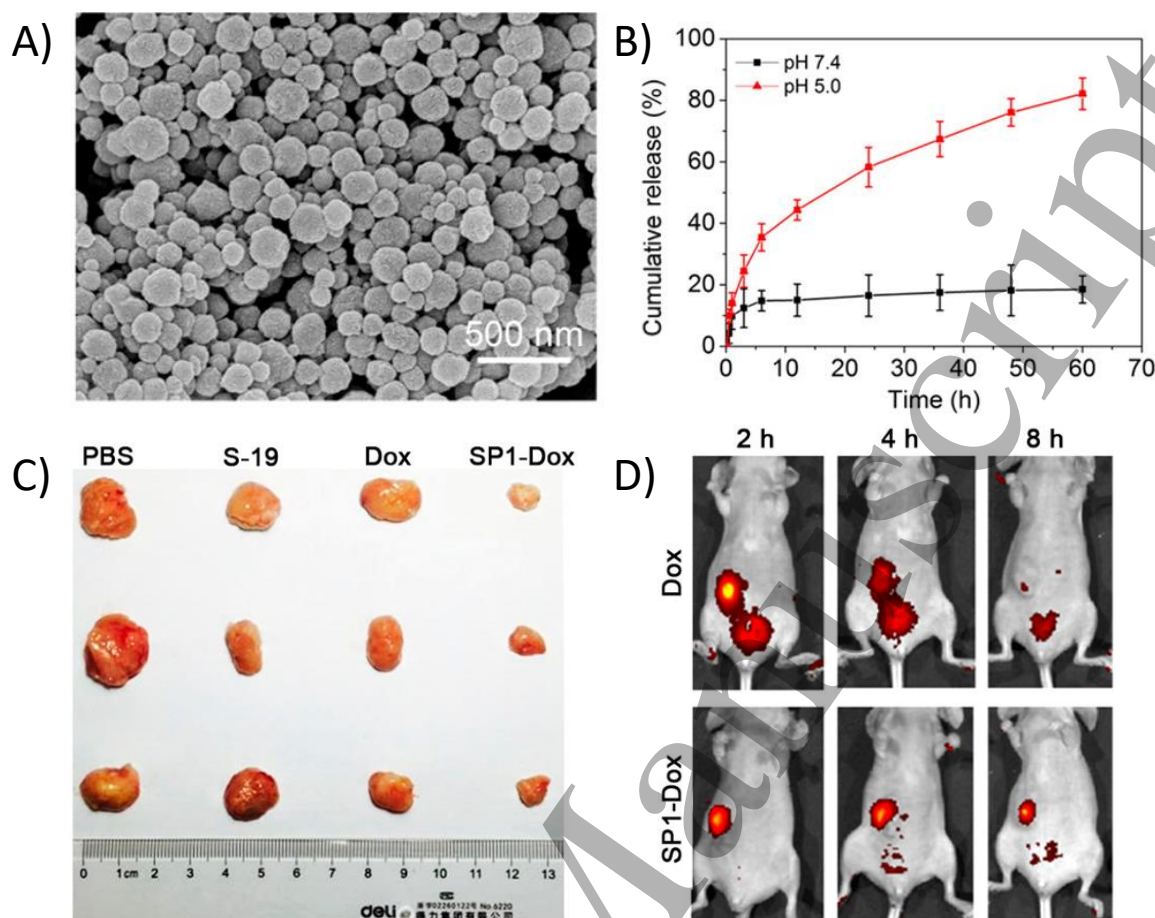


Figure 2 Structure characterization, in-vitro, and in-vivo studies of the S-19 NPs. A) SEM images of S-19 NPs prepared by salting out at 250 mM of KCl solution. B) Doxorubicin release from SP1 NPs at PBS solution (pH 7.4) or acetate buffer solution (pH 5.0) at 37° C. The data represent mean \pm SD (n=3). C) The image of the tumors dissected from tumor-bearing mice treated with the indicated formulation at the 22th day after the first injection. (D) In vivo fluorescence imaging of tumor-bearing mice treated with free Dox or SP1-Dox formulation. Different tumor-bearing mice were injected with the indicated formulation via peritumoral injection, and the mice were subjected to live imaging at the predetermined time point. Reprinted with permission¹¹¹. Copyright 2017, American Chemical Society.

2.2 β -sheet forming peptides

The β -sheet has been another widely used building motif for driving the self-assembly of peptides, driving the self-assembly of a large variety of nanostructures such as ribbons^{106,107}, nanotubes^{108,109}, monolayers with nanoscale order¹¹⁰, and nanoparticles¹¹¹. The β -sheet consists of several β -strands that are connected laterally by at least two or three backbone hydrogen bonds, forming a generally twisted, pleated sheet in a parallel or anti-parallel pattern¹¹². NPs can be generated and stabilized by the formation of the nanoconfined β -sheet structure enabling the possibility for drug delivery¹¹¹. Further studies^{113,114} incorporated polar zippers between neighboring β -strands via side-chain

stability and also limits the expansion of a larger β -sheet structure.

A recently discovered structural protein called ‘suckerin’, which is generated from Jumbo squid sucker ring teeth can self-assemble into a robust supramolecular network containing a high number of β -sheets as load-bearing nanoscale building blocks^{115,116}. Ping *et al.* generated an artificial suckerin-19 (S-19) through recombinant protein expression and fabricated suckerin NPs (SP1) through a salting-out method in the potassium chloride solution¹¹¹, with β -sheet structure stabilizing the NPs. The morphology and dimension of the NPs were examined via scanning electron microscopy (SEM) (Figure 2A). Doxorubicin, an anti-tumor drug, was incorporated in the NPs through diffusion, and in-vitro release was then conducted under various pH conditions

for a period of 60 hours. The release profile shown in Figure 2B showed a pH-dependent sustained release between pH 5.0 and pH 7.4. An *in vivo* antitumoral efficacy study was conducted for 21 days on a tumor-bearing nude mice model, and the SP1 showed enhanced retention of doxorubicin at the tumor site compared to free doxorubicin, thereby inhibiting tumor growth more effectively (Figure 2C-D). In addition, S-19 is also able to complex DNA into NP complexes mostly through non-electrostatic interactions and to induce DNA condensation during inter- and intramolecular β -sheet supramolecular assembly. Besides peptides that form NPs, Wang *et al.*¹¹⁴ designed a short amphiphilic peptide (Ac-

$I_3XGK-NH_2$ (X = Gln, Ser, Asn)) with a polar zipper between β -sheets rather than between β -strands, which in turn regularized the β -sheets into large flat ribbons. As previously reported, the peptide with sequence Ac-I₃K-NH₂ can assemble into flexible, twisted fibers with high stability owing to the hydrophobicity of Ile (I) and β -sheet formation¹¹⁷. The insertion of another X and glycine (G) residue in the middle of the sequence appears to form polar zippers between the β -sheets, which promoted the assembly of highly organized ribbons. Other recent studies on β -sheet-based nanostructures have been well summarized in other published review articles^{90,118,119}.

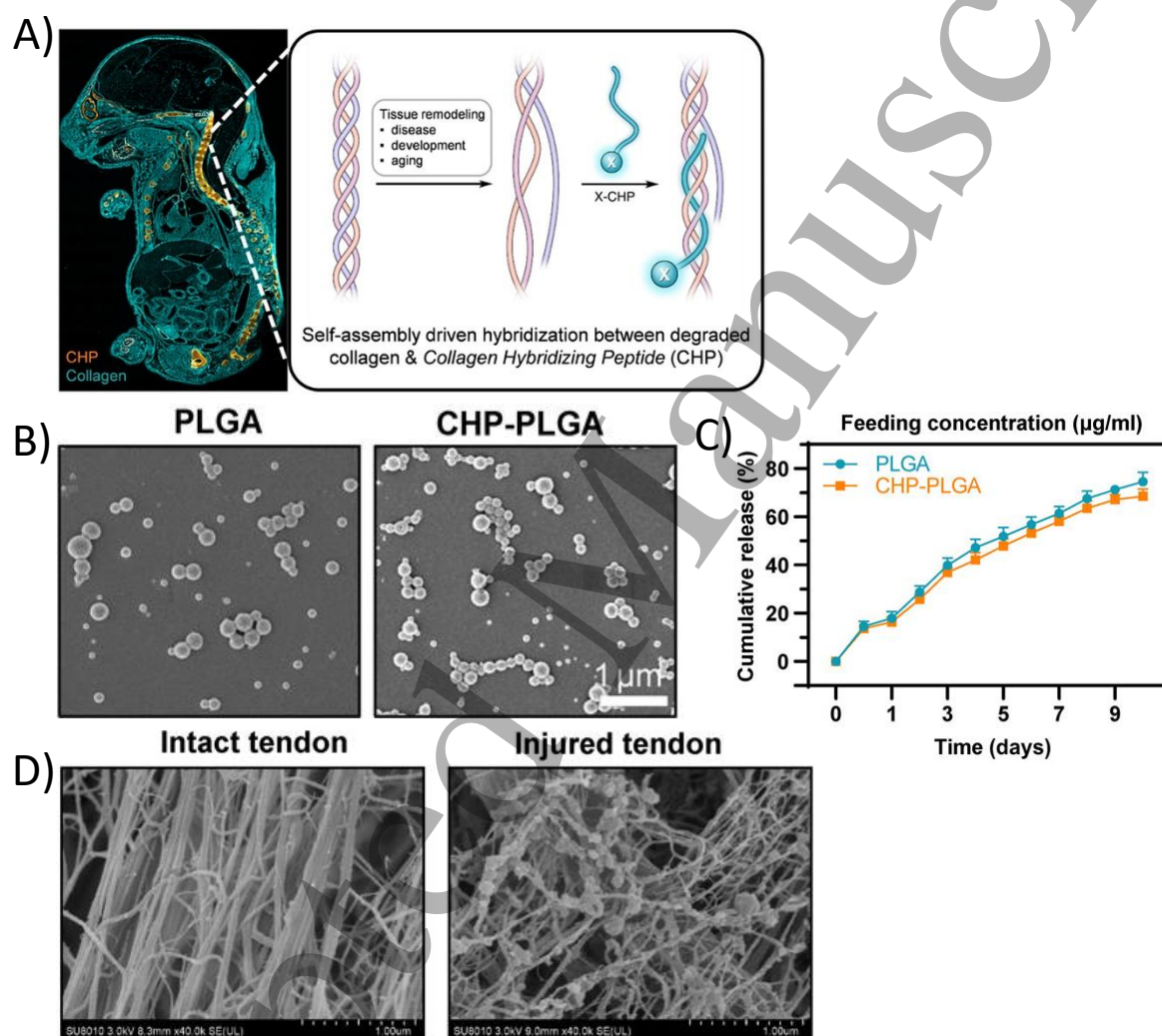


Figure 3 Confirmation of the CHP-PLGA collagen-binding. **A)** Left panel: Localization of CHP binding in a sagittal section of an 18 d.p.c. mouse embryo (E18) double stained with B-CHP (detected by AlexaFluor647-streptavidin (showed in orange) and an anti-collagen I antibody (detected by AlexaFluor555-labeled donkey anti-rabbit IgG H&L (showed in cyan); Right panel: Schematic of a CHP strand (labeled with X, X represents the biotin or fluorescent tag) hybridizing to denatured collagen chains and forming a collagen triple helix; **B)** SEM images of PLGA and CHP-PLGA nanoparticles. Scale bars, 1 μ m; **C)** RAPA release from PLGA and CHP-PLGA nanoparticles over the course of 10 days, n=4; **d)** SEM of CHP-PLGA binding to intact and injured tendon. A) is reprinted with permission²⁸. Copyright 2017, American Chemical Society. B-D) are adapted with permission¹²⁷. © The Authors, some rights reserved, exclusive licensee AAAS. Distributed under a Creative Commons Attribution NonCommercial License 4.0 (CC BY-NC)

2.3 Triple helical peptides (Collagen-mimetic peptides)

Collagen is the most abundant protein in the human ECM, providing both mechanical integrity and interactions with cell-surface integrins for adhesion. Collagen-mimetic peptides (CMPs) (or collagen-like peptides, CLPs) are short synthetic versions of the native collagen that have been widely employed in the generation of peptide-based materials. CMPs are composed of three peptide chains where each CMP chain comprises multiple repeats of amino acid triplets, (X–Y–G), where X and Y are usually proline (P) and hydroxyproline (O), respectively¹²⁰. The three CMP chains each individually adopt a polyproline II helix structure and then self-assemble via a combination of stereoelectronic effects and hydrogen bonding between adjacent chains to form the CMP triple helix which, at temperatures below the melting temperature (T_m) of the triple helix, mimics the triple helical structure of native collagen¹²⁰. As first reported by Li *et al.*, the collagen-hybridizing peptide (CHP) (single strand of the CMP triple helix) is able to bind with high stability to partially denatured collagens through a strand invasion process¹²¹. Therefore, for decades, short CMPs have been used in thermo-responsive fabrics¹²², 3D-scaffolds¹²³, and as therapeutic matrices and molecules owing to their collagen-binding and heat-triggered folding-unfolding behavior¹²⁴.

Inspired by the natural collagen fiber structure, many studies have been conducted to incorporate CMPs as building blocks for constructing highly ordered nanostructures⁴. Koga *et al.* functionalized the N-terminus of CMP with aromatic rings, which built rod-like micelle fibers with the capability to

encapsulate hydrophobic molecules¹⁰. San *et al.* built a novel nanofiber by self-assembling a peptide that incorporates both β -sheet and triple-helical motifs which is CMP¹²⁵. This nanofiber showed excellent affinity to denatured collagen by multivalency effects attributed to the surface CHP, at the same time, can be shortened to less than 100 nm to avoid most of the partition into dermal tissue after the injection into normal mice. Besides the assembly into fibrillar structures, CHPs also show high collagen affinity. Recent work conducted by Hwang *et al.* showed the possibility of utilizing a fluorescein-labeled CHP as a marker to bind denatured collagen for probing damaged tissue²⁸ (Figure 3A). In contrast to antibodies, the CHP demonstrates no species conflicts with tissue samples or with other primary antibodies, enabling facile double staining of tissues. Additional work conducted by Zitnay *et al.* utilized the CHP as a quantitative probe to measure collagen molecular damage during tendon cyclic fatigue loading¹²⁶. Other pioneering work conducted by Chen *et al.* reported a rapamycin (RAPA) delivery system using CHP modified poly (lactic-co-glycolic acid) (PLGA) NPs (NP morphology shown in Figure 3B) to specifically target pathological collagen in tendon for heterotopic ossification (HO) suppression¹²⁷. Compared to the injection of traditional drugs, the CHP-PLGA-RAPA NPs showed not only excellent targeting ability (specific binding SEM data shown in Figure 3D) but also the sustained-release ability of RAPA with high bioactivity (the in-vitro release study is shown in Figure 3C). Very recent work reported by Kessler *et al.* applied peptoids with 7 different functional groups as substitutions for proline in a CMP-based peptide, without a reduction of

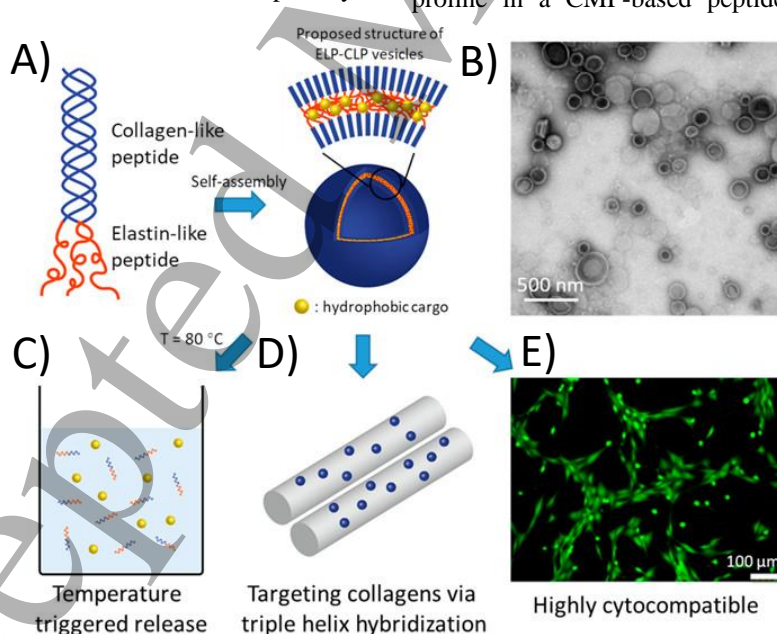


Figure 4 Versatile properties of the ELP-CLP NPs. A) Self-assembly process of ELP-CLP sequences. B) TEM confirmation of vesicle morphology. C) Thermal-responsive release of hydrophobic molecules. D) Targeted binding to denatured collagen is attributed to the CLP of the outer layer. E) Live/dead fluorescence images of 1000 $\mu\text{g/mL}$ vesicles in culture with NIH-3T3 fibroblastic cells. Reprinted with permission⁷⁶. Copyright 2017, American Chemical Society.

thermal stability¹²⁸. This discovery broadens the ways for functionalizing CMPs thus enabling essentially countless possibilities for CMP modifications.

2.4 Amphiphilic peptides with alkyl tails and co-peptides

The amphiphilic peptide is one of the most extensively studied and successful platforms for self-assembling peptides in regenerative medicine. In general, amphiphilic peptides contain a hydrophobic tail and a hydrophilic head, where the hydrophobic tail is sequestered as the core of the assembled structure and the hydrophilic head is localized on the surface. These peptides self-assemble to form a large variety of morphological structures with nano-dimensions such as micelles^{129,130}, vesicles^{9,131}, or sheets⁸. Tsonchev *et al.* demonstrated that the self-assembly of amphiphilic peptides is driven by both hydrophobic as well as electrostatic interactions¹³². In this section, we focus mainly on amphiphilic peptides with alkyl groups or those comprising co-polypeptides.

As a traditional hydrophobic motif, alkyl groups can be conjugated as a 'tail' for hydrophilic peptides thus enabling self-assembly via inter- and intra-molecular interactions^{133,134}. Fry *et al.* designed a peptide-alkyl amphiphile system containing two different charged amino acids (histidine and lysine) and an alkyl tail (C8, C12, C16, or C18), which self-assembled into nanofibers with quantitative pH responsiveness¹³⁵. Chensinin-1b, an antimicrobial peptide, has been conjugated to an alkyl tail (C8, C12, or C16), as reported by Dong *et al.*, to create an amphiphile sequence containing chensinin-1b peptide that self-assembles into a micellar structure in aqueous solution with cell penetration ability and up to 7-fold anti-cancer activity by the incorporation of the aliphatic acids¹³⁶. Unlike the tail-insertion

of the alkyl group, a recent study conducted by Yaguchi *et al.* reported several peptide chains that contained centrally located alkylene groups of different lengths (C1, C2, C3, and C4) in the peptide via solid-phase peptide synthesis¹³⁷. Comparing the physicochemical properties of those sequences, they found that the central alkylene chain allowed for strengthened hydrogen bonds in the antiparallel β -sheet stacks, in which the amphiphilic molecule showed great potential to self-assemble into nanofibers and stiff hydrogels with low cell adhesion. Song *et al.* designed another amphiphile applying the alkyl group in both the middle and the tail of the peptide chain, which formed into well-organized twisted ribbons and flat ribbons owing to antiparallel and parallel β -sheet arrangements, respectively¹².

Luo *et al.* designed an amphiphilic co-peptide which contains a hydrophobic domain comprising an elastin-like peptide (ELP) and a hydrophilic domain comprising a collagen-like peptide (CLP) with the sequence (VPGFG)₆-b-(GPO)₄GFOGER(GPO)₄GG⁹. With a simple annealing process, this ELP-CLP conjugate can easily self-assemble into a bilayer vesicle structure with quantitatively measured dual thermo-responsiveness (Figure 4A-B). Fine-tuning of the thermo-responsiveness was further studied and revealed^{8,138,139}. The ability to encapsulate hydrophobic molecules (Figure 4C), to target denatured collagen (Figure 4D), and to show cytocompatibility has been further tested in additional studies⁷⁶, in which showed a sustained release for over 3 weeks as well as high cytocompatibility with both NIH-3T3 fibroblasts and ATDC5 chondrocytes (Figure 4E). Considering the relative chain length of the individual peptide domains plays a key role in the self-assembly process, and Qin *et al.* further revealed the relevance between the self-assemble morphology and the relative length of two domains with the

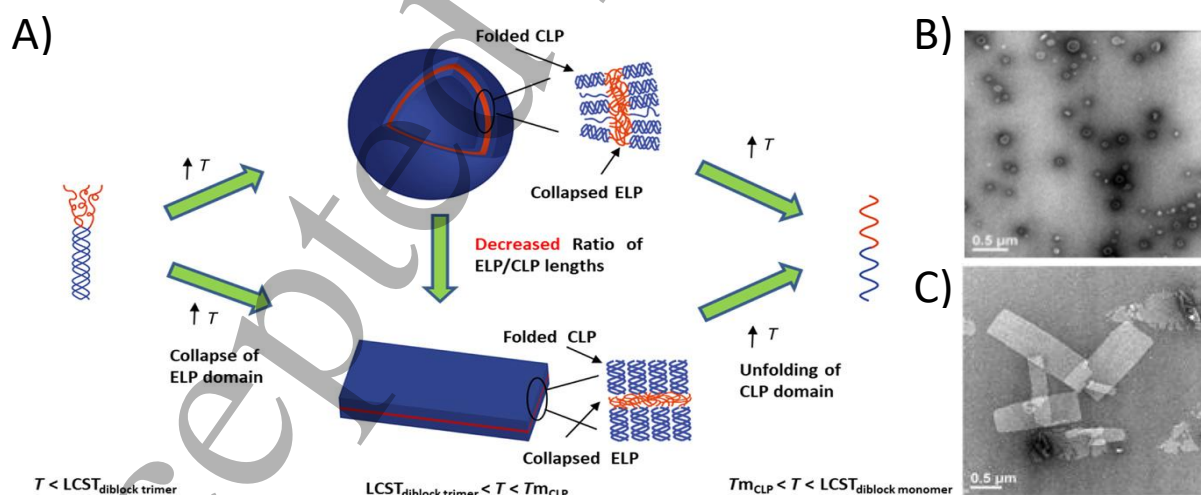


Figure 5 Tunable morphology of the ELP-CLP NPs. A) Proposed assembly/disassembly and bilayer structure of the ELP-CLP vesicles and platelets, owing to different hydrophobic volume of the inside ELP layer. TEM images of B) vesicle and C) platelet structures. Adapted with permission⁸. © The Authors, some rights reserved, exclusive licensee AAAS. Distributed under a Creative Commons Attribution NonCommercial License 4.0 (CC BY-NC)

sequence $(VPGWG)_2(VPGFG)_x-b-(GPO)_yGG^8$. With a shortened hydrophobic ELP domain or elongated hydrophilic CLP domain, the ELP-CLP conjugates self-assembled into a nanoplatelet structure instead of the original vesicle structure, in which it can also be quantitatively tuned around the ELP/CLP length ratio (ca. 0.50) (Figure 5). Similar discussions on the morphology change resulting from the different ratios of the hydrophobic and the hydrophilic domain in polymer amphiphiles have been ongoing for decades¹⁴⁰⁻¹⁴², and the inclusion of additional peptide-based domains offers opportunities to expand the structures and functionalities of the nanostructures.

2.5 Short peptides

Studies have also shown that very short peptides can self-assemble into a variety of nanostructures such as NPs, nanofibrils, and nanoribbons, thus minimizing the cost and difficulty of their synthesis and at the same time, increasing their relative stability. These short peptide fragments were identified largely from studies aimed at elucidating the minimum required sequence for amyloid formation¹⁴³. As a well-studied example, NFGAIL (hIAPP22-27) is a hexapeptide fragment of the islet amyloid polypeptide (IAPP) that forms well-ordered amyloid fibrils similar to those formed by the full-length polypeptide¹⁴⁴. In some cases, even a single amino acid with certain modifications can self-assemble into nanostructures such as nanofibrils^{145,146} or into hydrogels¹⁴⁷. In this section, we focus mainly on recent reports of nanostructures comprising very short peptides.

The design of peptides with fewer amino acids has been a subject of significant study. Sequences such as $Ac-A_mK_n-NH_2$ and $Ac-I_mK_n-NH_2$ have been identified¹⁴⁸, which have the ability to self-assemble into nanofibers, nanoplatelets, and nanoribbons. Because of the short chain length of those peptides, the substitution of only two to three amino acids can

dramatically manipulate the self-assembly process, thus resulting in completely different assembled morphologies. For example, the sequence $Ac-I_3K-NH_2$ can self-assemble into nanofibers through β -sheet formation, however, when leucine (I) is replaced with isoleucine (L), the sequence $Ac-L_3K-NH_2$ will self-assemble into spherical NPs¹⁴⁸. With subtle tuning of this sequence by replacement of the terminal lysine (K) with arginine (R) or histidine (H), helically coiled, twisted or flat nanoribbons can be formed, respectively, attributed to the different stacking styles of the β -sheet monolayers caused by hydrogen bonding between the peptide backbones¹⁴⁹. As previously described, work conducted by Wang *et al.* utilized this sequence, and with the insertion of two polar amino acids, a multi-layer was produced, presumably via hydrogen bonds between polar amino acids both above and below the plane of the β -sheets (i.e., a polar zipper)¹¹⁴.

Tripeptides have also gained much attention recently. Glossop *et al.* designed a tripeptide sequence D-Dab/Lys which supported self-assembly of highly entangled nanofibrillar networks and also exhibited substantial antimicrobial activity against *Staphylococcus aureus*¹⁵⁰. Another study used aromatic amino acids such as tyrosine or phenylalanine, and/or negatively charged amino acids, such as aspartic acid, to build a tripeptide sequence, in which the relative position of these three amino acids was manipulated, resulting in the self-assembly of nanostructures with distinct morphologies, such as nanofibrils and nanoribbons¹⁵¹ (Figure 6). These approaches increase the control and tuning of the properties of the materials, and the production of the short peptide enables facile scale-up.

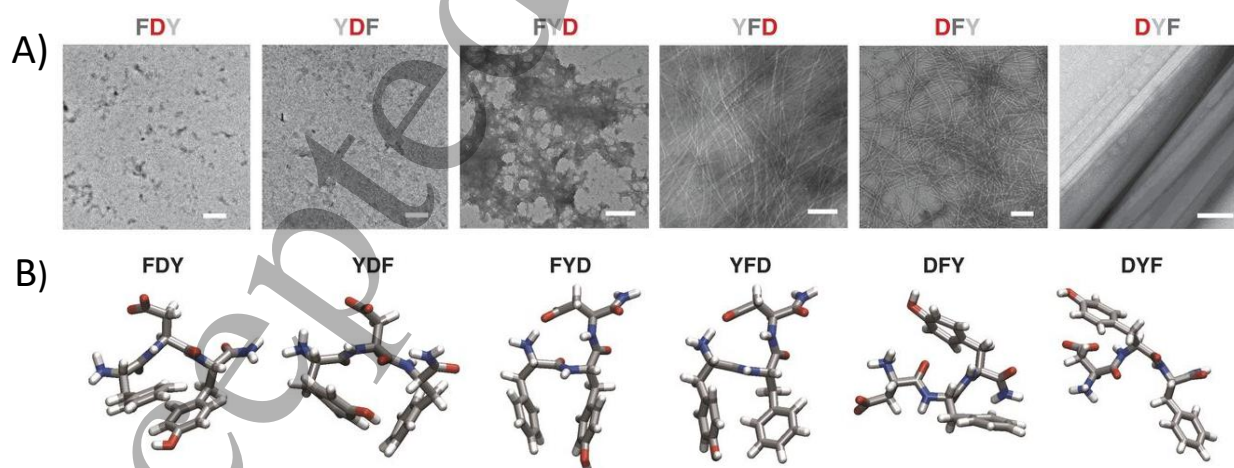


Figure 6 Defined morphologies with different arrangements of amino acids and the peptide backbones. A) TEM micrographs of structures formed by self-assembly of tripeptides. Scale bars: 100nm; B) Preferred conformations for each peptide via molecular dynamic (MD) simulation. Adapted with permission from the AAAS¹⁵¹. Copyright 2017, AAAS.

Dipeptides are one of the simplest building blocks in peptide nanotechnology¹⁵². Among these, the diphenylalanine peptide (L-Phe-L-Phe; FF) is perhaps the most famous and also the core recognition motif of the Alzheimer's β -amyloid peptide^{152,153}. Many studies indicated that this peptide and its derivatives can self-assemble into highly ordered nanostructures such as NPs and nanoribbons^{154,155}, or nanoscale matrices such as hydrogels¹⁵. In the FF dipeptide system, the main driving force of the structure self-assembly is the hydrophobic interaction and the π - π interaction. Work conducted by Schnaider *et al.* showed that the FF dipeptide

analyzing the real-time assembly, they managed to find the length and the diameter as a function of time showing a linear trend of growth during the first 200 seconds. The assemblies elongated in an axial growth pattern to approximately 2000 nm while they widened in a radial pattern to approximately 250 nm. This study also demonstrated that LCTEM can be a useful tool for studying the self-assembly and dynamics of a wide range of soft materials and biological systems such as organic small molecules, amyloid fiber formation and inhibition, and cellular types of machinery such as actin filaments and microtubules.

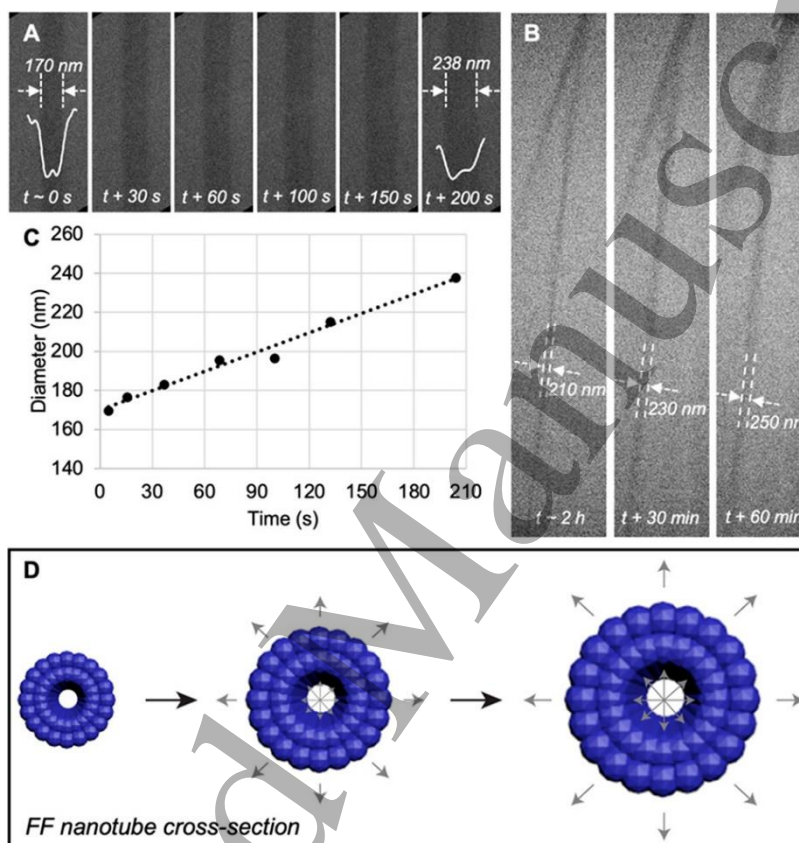


Figure 7 Radial growth of FF nanotubes by LCTEM. FF monomers were added to deionized water, placed in the liquid-cell, heated at 80 °C for 1 h, and allowed to cool to room temperature for 30 min. (A and B) LCTEM snapshots of radial growth of FF nanotube with integrated line profiles illustrating the increase in tube diameter and hollowness of the nanotube. Data acquired with an instantaneous flux of $0.3 \text{ e}^- \text{ \AA}^{-2} \text{ s}^{-1}$. C) Outer diameter plotted as a function of time shows the linear trend in increase in diameter. D) Schematic of FF nanotube cross-section illustrates the association and dissociation events leading to the increase in tube diameter with time. Reprinted with permission¹¹. Copyright 2021, American Chemical Society.

was able to self-assemble into nanofibers and had higher bactericidal activity than non-assembled Gly-Gly (GG) or FF sequences²³. Although the FF dipeptide has been a subject of investigation for multiple decades, direct experimental evidence of the assembly process in real-time has remained elusive. A recent study conducted by Gnanasekaran *et al.* utilized liquid-cell transmission electron microscopy (LCTEM) to monitor the dynamics and the growth of the FF dipeptide assemblies at nanometer resolution¹¹ (Figure 7). By

3. Biomedical applications

For decades, nanoscale structures such as polymersomes and liposomes were designed to self-assemble for biomedical applications including serving as drug delivery carriers¹⁵⁶, nanoreactors¹⁵⁷, and magnetogels¹⁵⁸. However, many of those showed a certain degree of cytotoxicity thus limiting their potential for clinical use. For example, positively charged

liposomes are known to cause severe immune responses¹⁴³ and polymeric NPs can increase the risk of particle aggregation and toxicity⁸¹. Liposomes and lipid-based NPs have been discovered and commercially available for drug delivery systems for decades. However, they present several technological limitations such as high production cost, leakage and fusion of encapsulated drugs, oxidation and hydrolysis reaction of the phospholipid, and short half-lives¹⁵⁹. Polymer-based systems have been explored as a means to improve cellular uptake, but the surface functionalization can be complex and inefficient, and unwanted immune responses are another obstacle that cannot be easily bypassed.

Peptide self-assembled nanostructures with various dimensions and morphologies have been developed and utilized for many biomedical applications such as tissue regeneration, biosensors^{160,161}, and bioimaging^{162,163}. Owing to their bio-inspired nature and efficient production, they can be good candidates for drug or gene delivery^{67,68,127,154}, as they can be designed to target specific cellular components and can be equipped with functionalities that are sensitive to external and internal stimuli. For example, certain peptide-based nanostructures comprising cell-penetrating peptides (CPPs) can reduce cytotoxicity and increase cellular uptake¹⁶⁴⁻¹⁶⁶. We review some recent encapsulation studies and efforts to modify cellular uptake and intercellular trafficking.

3.1 Drug encapsulation and stimuli responsiveness

Despite the longstanding and widespread use of small molecule drugs, efforts to improve the bioavailability and stability of the drugs have remained of interest in order to improve targeting and reduce necessary dosages. For example, dexamethasone is one of the most frequently used glucocorticoids for anti-inflammatory treatments⁷¹ and is also considered one of the safest. However, the low bioavailability resulting from the low solubility of drugs limits the dosage, especially confined for diseases that require a higher dosage of drugs. Furthermore, serious side effects have been recorded mostly because of its low water solubility and low bioavailability, which have in select cases resulted in precipitation *in vivo*¹⁶⁷.

Also, there are many cargo molecules such as RNA, DNA, hydrophilic drugs such as methotrexate, and hydrophobic drugs such as paclitaxel, that require a carrier to stabilize the drug and/or increase bioavailability while in the physiological environment. From Doxil[®], the first FDA-approved nanodrug (1995), to the most recently commercialized COVID-19 RNA-delivery vaccine (2020), three decades of nano-drug development have clearly demonstrated the advantages and necessity to develop medicines that are improved via their incorporation into nano-sized carriers. Although approximately 50 nanomedicine carriers have been American Food and Drug Administration (FDA)-approved since Doxil[®] in 1995, only 2 of them are protein-based¹⁶⁸

(although there are more than 80 FDA-approved therapeutic peptides¹⁶⁹), and the opportunities for protein- or peptide-based nanomedicine carrier promises new discoveries.

Many approaches to encapsulating drugs in nanostructures have been reported¹⁷⁰⁻¹⁷², and essentially all employ physical encapsulation and/or chemical modification. Physical encapsulation or physical adsorption is mainly based on the noncovalent interactions between the cargo and the carrier, including but not limited to π - π interaction, hydrogen bonding, and ionic interactions¹⁵⁶. The main advantage of physical encapsulation is that cargos don't need to be functionalized to be encapsulated thus broadening the choices of cargo and reducing toxicity during production. However, weak non-covalent bonds can result in rapid clearance of the cargo and the carrier, thus decreasing dosing efficiency. The chemical encapsulation, on the other hand, owing to the strong covalent bonding between the cargo and the carrier, has the ability to withhold the cargo for a longer period for sustained retention^{156,173}. The encapsulation amount can also be tuned by simply changing the amount of the reagent, which grants flexibility for the loading of the cargo, although potential modification of drug efficacy and toxicity are also potential challenges.

Besides the encapsulation of the drugs, their release is a key factor to consider when developing nanomedicine. Diffusion of drugs from carriers is the most traditional and fundamental way to accomplish the task, whereas the uncontrolled leak of drugs remains the primary limitation. Inspired by the stimuli-responsive polymers (SRPs), a peptide that reacts to stimuli has been developed. Similar to SRPs, the process has similar stimuli-responsiveness including but not limited to pH-responsiveness, temperature-responsiveness, redox-responsiveness, photo-responsiveness, and ion responsiveness¹⁷⁴. In order to gain much more precise control on the release of drugs, several stimuli-responsive polypeptides have been fabricated¹⁷⁴⁻¹⁷⁶. Although a large variety of SRPs has been approved by the FDA, such as thermal-responsive poly(N-isopropyl acrylamide) (pNIPAM) and pluronic F127 (PF127), there are no polypeptide formulations that have yet been approved for thermal-responsive applications.

3.2 Enhanced cellular uptake

One of the most desirable properties of drug nanocarriers is the ability to bind specifically to the desired site of the cell membrane or the molecules of interest, and peptides are particularly effective in this regard. Although nano-sized structures are of appropriate size for cell entry and have the ability to encapsulate drugs, without a proper way to gain entry to the cell, the encapsulated drug efficacy will be minimized. For example, the peptides RGD and NTFR have been used to bind fractalkine and 8 different integrins^{177,178}. Studies have found that certain types of peptides such as gastrointestinal

peptides, insulin, pituitary adenylate cyclase-activating polypeptide (PACAP), and vasoactive intestinal peptide (VIP)¹⁷⁹ can be useful for crossing or assisting nanostructures to cross physiological barriers, such as the blood brain barrier (BBB)⁷⁷. Functionalization of nanostructures such as liposomes with these peptides can also greatly improve membrane binding and penetration. Also, the self-assembly process plays an important part in the cellular uptake, for the

physical and chemical properties of the NPs such as dimension (less than 200 nm), morphology (normally spherical), surface charge (positively charged), and particle membrane elasticity (more rigid) can significantly affect the efficiency of the uptake.

3.2.1 Targeted binding. For achieving enhanced cell uptake via targeting, peptides have been used to promote the

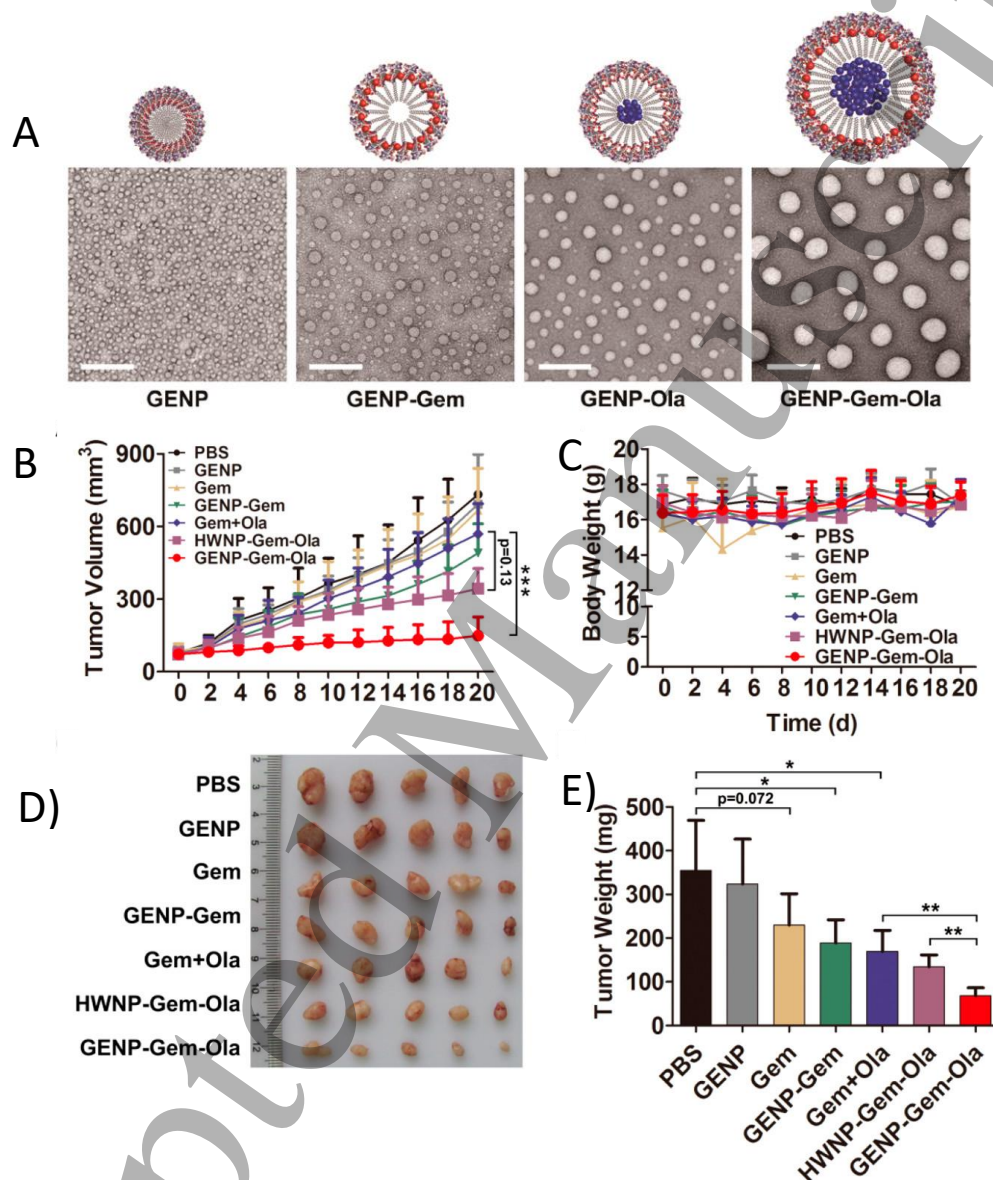


Figure 8 Tunable morphologies of the GENPs and the in-vivo applications. A) Schematic diagram of the change of nanoparticles' morphology after drug loading (top row); The morphology of GENP, GENP-Gem, GENP-Ola, and GENP-Gem-Ola was assessed using TEM (bottom row); B) Tumor growth curves. Nude mice bearing capan-1 human pancreatic tumors, implanted 2 weeks prior to the commencement of treatment, received intravenous injections of PBS, GENP, Gem, GENP-Gem, Gem+Ola, HWNP-Gem-Ola, or GENP-Gem-Ola every other day at a Gem dose of 5 mg/kg and an Ola dose of 50 mg/kg; * $p < 0.05$, *** $p < 0.001$; C) Body weights of the mice were recorded every 2 days throughout the treatment period; D) Gross morphological appearance of the tumors at the end of the treatment period; E) Tumors' weights at the end of the treatment period; $n = 5$ for each group in (b) and (e); * $p < 0.05$, ** $p < 0.01$, *** $p < 0.001$. Reprinted with permission¹⁸¹. Copyright 2018, American Chemical Society.

improved accumulation of drugs in the target tissue and to increase the dosing efficiency. Of these, RGD has been a traditional peptide motif used for cell targeting over the past 30 years¹⁸⁰, and it plays an important role in cancer therapy. Fan et al. functionalized a fluorescent cyclic-peptide-based NP (cyclo[-(D-Ala-L-Glu-D-Ala-L-Trp)₂-]) with RGD and physiologically encapsulated epirubicin (EPI) for esophageal cancer (EC) treatment¹³. Human esophageal cell lines were used to test the selectivity binding of these RGD-fluorescent NPs with EPI (RGD-f-PNPs/EPI) to the $\alpha v\beta 3$ integrin. The RGD-f-PNP/EPI also showed an increased in-vitro release of EPI in an acidic environment, which can benefit the in-vivo release in the acidic tumor environment. Further in vivo study showed the RGD-f-PNPs/EPI can suppress the tumor growth for 24 days with a significantly low dose (1.5 mg/kg) compared to the free EPI control (6 mg/kg) also with reduced dose-dependent damage to other organs. Furthermore, with the fluorescein embedded in the particle, the retention of the

particles inside the tumor tissues could be monitored using near-infrared fluorescent imaging. Both in vivo and in vitro experiments showed the great potential of this peptide-based fluorescent-labeled NP for real-time tumor imaging and targeting EPI delivery to tumor cells.

Another study performed by Du et al. developed an epidermal growth factor receptor (EGFR) targeting, with GE11 peptide, self-assembled amphiphilic peptide nanoparticle (GENP), comprising the peptide GE11, which is equipped with a hydrophilic 12-amino-acid sequence with tested powerful EGFR-binding efficiency and a hydrophobic octadecanoic acid molecule (C18) as the tail. These particles were utilized to co-deliver gemcitabine (Gem) and the poly-ADP-ribose polymerase inhibitors (PARPi) olaparib (Ola) to kill BRCA2 mutant pancreatic cancer (PCa) capan-1 cells¹⁸¹. A core-shell self-assembly was fabricated with C18 as the hydrophobic core and the GE11 as the EGFR-binding shell. (Morphologies were confirmed via TEM shown in Figure 8A).

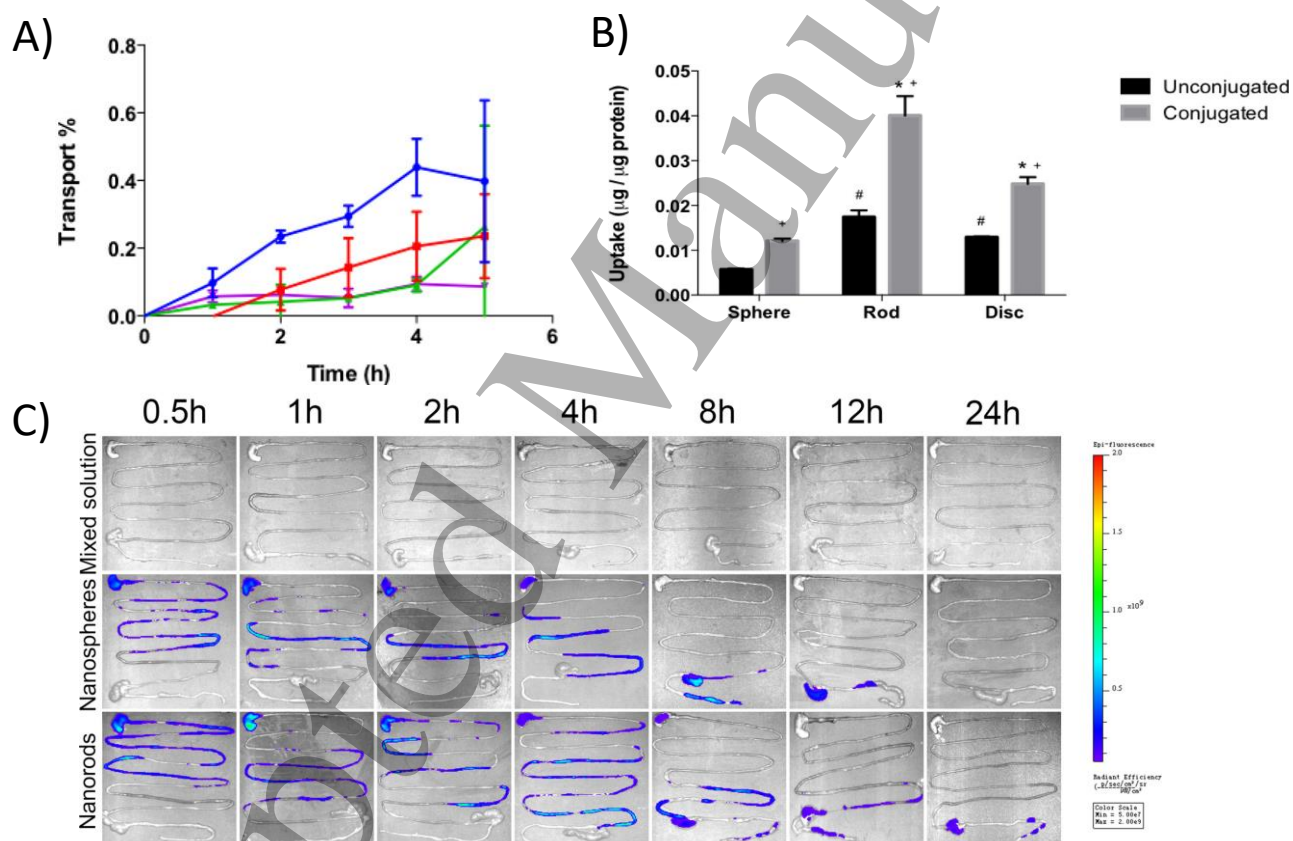


Figure 9 Statistical and visual confirmation on the cellular uptake of different NPs. A) Transport of nanoparticles across Caco-2/HT-29 cells. Different particle diameters are represented as blue circles (50 nm), red squares (200 nm), green upright triangles (500 nm) and purple downward triangles (1000 nm); B) Uptake of unconjugated and biotin conjugated nanoparticles by Caco-2/HT-29 cells. Uptake of unconjugated (black bars) and biotin conjugated (grey bars) nanoparticles by Caco-2/HT-29 cells. Biotin conjugation significantly improved uptake of particles of all shaped particles in Caco-2/HT-29 cells; while biotin conjugated, and unconjugated rods and discs demonstrated higher uptake than conjugated and unconjugated spheres respectively; C) Typical pictures of gastrointestinal segments from SD rats after ex vivo imaging and quantification of nanoparticles in stomach. A) and B) are adapted and reprinted with permission from Elsevier¹⁹³. C) is reprinted with permission⁵². Copyright 2018, American Chemical Society.

Both *in vivo* and *in vitro* studies showed strong binding to cells that exhibit a high level of EGFR (capan-1 PCa cells) and selective accumulation in capan-1 tumor xenograft in mice (Figure 8B-E). The encapsulated Gem and Ola work synergistically to inhibit the growth of BRCA2 mutant capan-1 cells *in vitro* and capan-1 derived tumors *in vivo*. Moyer *et al.* also developed a peptide-based nanofiber that can target death receptor 5, to encapsulate paclitaxel (PTX) for cancer therapy¹⁸².

3.2.2 Physicochemical properties of NP on cellular uptake. Many parameters (morphology, dimension, surface charge, and elasticity) of the nanoparticles directly affect uptake efficiency, the endocytotic route, as well as cytotoxicity. The biggest advantage of the NPs with respect to cellular uptake is their nanometer-scale size, and this is a key factor mediating cellular uptake efficiency as well as cytotoxicity. In drug delivery applications, one of the main goals is to prolong the retention time of the NP in the blood by preventing the NPs from being removed by the reticuloendothelial cells. In this case, increasing the size will result in a faster removal rate^{183,184}. Several studies have indicated that 50 nm NPs have the highest cellular uptake efficiency, while larger or smaller particles will have decreased uptake efficiency^{185,186}. Studies have also shown that NPs sized less than 200 nm^{78,187,188} will more easily be trafficked through clathrin- and caveolin-mediated endocytosis pathways, with caveolin-mediated pathways preferred for NPs smaller in size compared to those that are trafficked through clathrin-mediated pathways. Ho *et al.* found that 20 and 40 nm polystyrene NPs (PS NPs) are more dependent on caveolin-mediated endocytosis than 100 nm PS NPs in HUVEC cells¹⁸⁷. A similar trend has also been observed in another study where the caveolin-mediated endocytosis dominated the uptake of 50 nm gold NPs for HepG2 cells.¹⁸⁹

Besides NP size, both the shape and the orientation of the NP relative to the cell membrane can impact cellular uptake. Studies have shown that in many cases, spherical NPs have more efficient cellular uptake than rod-like structures¹⁹⁰. For example, one study¹⁹¹ showed that ten-fold more filomicelles can remain in the circulation than spherical counterparts, as the spherical filomicelles are internalized by the cells more rapidly than longer filaments. By comparing the uptake of the star, triangle, and rod-like structures, Xie *et al.* found high internalization efficiency of rod structure on RAW267.4 macrophage and low efficiency of star structure owing to the multiple branches¹⁹². Banerjee *et al.* presented a recent study on the role of NP geometry and surface chemistry in uptake and transport *in vitro* across different intestinal cell monolayers (Caco-2/Raji-B/HT29)¹⁹³. They found not only those smaller particles show higher uptake (Figure 9A), but also that rod-like and disc-like NPs have two-fold higher

intestinal cellular uptake efficiency than spherical NPs (Figure 9B), which make them good candidates for oral drug delivery carriers. Further studies conducted by Li *et al.* confirmed the identical trend when being applied *in vivo* through lymphatic delivery where nanorods were observed to be transported by lymph to a higher extent than nanospheres (Figure 9C)⁵².

Another critical factor of the cellular uptake is the surface charge of the NPs. The cell membrane is usually negatively charged, which shows great affinity to cationic NPs, thus increasing cell uptake versus that of anionic or neutral NPs^{194,195}. For peptide-based NPs, arginine is the most used amino acid among the 20 natural amino acids and is used commonly in cell-penetrating peptides (CPP). Owing to their small size and penetration capability^{14,196}, CPPs such as TAT-based proteins, oligoarginines, and chimeric cell-penetrating peptides have been applied alone or in combination with other peptides to deliver therapeutic cargos to desired cells. CPPs are widely used as a treatment for different diseases and inflammation such as cancer^{164,165,197,198}, nervous system disorders¹⁹⁹⁻²⁰¹, otoprotective^{166,202}, and diabetes^{203,204}. CPPs-mediated nanoplatfoms such as CPPs-mediated quantum dots (QD) can also function as imaging agents for diagnosis. Studies showed that CPP-modified QDs not only possess the advantages of QDs, such as imaging ability but also have high cell membrane permeability^{42,205}. However, limitations remain as the CPPs have the potential to cause unwanted immune responses, potential cytotoxicity, endosomal degradation, and low penetration specificity¹⁴.

Lastly, elasticity is another physical property of the NPs that can impact the biodistribution, targeting, and cellular uptake efficiency. The elasticity is often described using the word 'rigid' or 'soft' as defined by Young's modulus, and recent work conducted by Guo *et al.* confirmed that the elasticity of the NPs can significantly affect the efficiency of the cellular uptake in human breast cancer cells (MDA-MB-231 and MCF7)²⁰⁶. They used nanolipogels (NLGs), which are composed of lipid bilayers around an alginate core with tunable elasticity. The Young's modulus of these NPs was determined by atomic force microscopy (AFM) and ranged from 0.045 MPa to 19 MPa. Rigid NPs can penetrate the cell membrane more efficiently than soft NPs through the endocytosis pathway, while soft NPs have higher penetration efficiency through diffusion-based pathways. Thus, they concluded that the particle modulus regulates the cellular uptake of drug delivery carriers via regulating cell internalization pathways. Similar work has also been conducted by Anselmo²⁰⁷ to test the cellular uptake efficiency of NPs with the different elastic modulus (0.255 kPa to 3 MPa) and similar results have been achieved with immune cells (J774 macrophages), endothelial cells (bEnd.3), and cancer cells (4T1). Furthermore, they discovered that with immune cells (J774 macrophages), this endocytosis process is even more pronounced.

3.3 Intracellular trafficking

After cellular internalization, NPs undergo transport and trafficking to various intracellular destinations. During this process, they will first encounter membrane-bound intracellular vesicles (early endosomes). The early endosomes will then ferry the NPs to the desired cellular destination before they turned into late endosomes, which will integrate with lysosomes to form endolysosomal vesicles and degrade the NPs trapped inside. To avoid the degradation of the NPs, certain modifications have been used to escape the endosomes. Even if the NPs make it to the final destination,

they still have to find their own way to target and bind to the organelles to achieve longer retention. Therefore, three different approaches can be used to modify the trafficking rates of NPs: 1) Improve the endosomal escape efficiency of the NPs; 2) Increase the targeting to organelles; 3) Decrease the exocytosis rate.

As briefly mentioned above, the first barrier that the NPs need to overpass is the endosomal barrier upon endocytosis. To avoid the degradation of the NPs via late endosomes^{186,208}, certain peptide-functionalized NPs have been used to escape endosomes altogether. Peptides that cause membrane destabilization or disruption have been increasingly used for

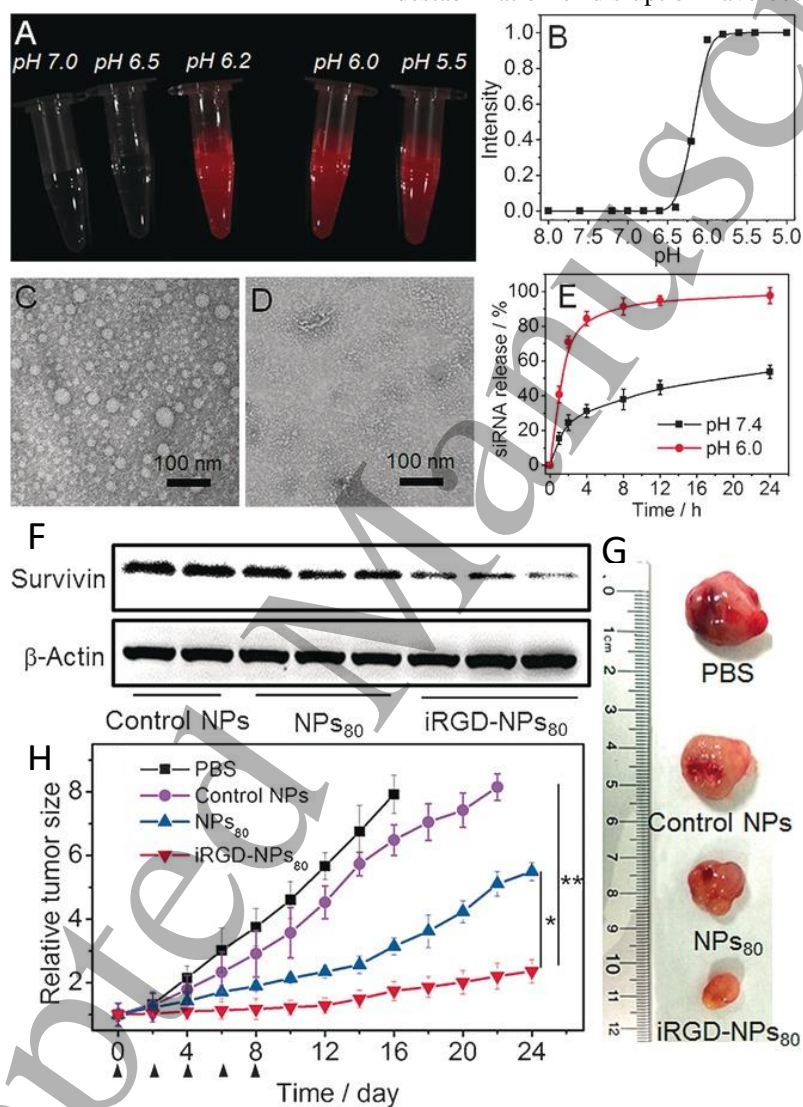


Figure 10 Encapsulation of si-RNA in a pH-responsive NP system with tumor-target ability. A) Fluorescent image of the Cy5.5-labelled NPs of PDPA80 at different pHs. B) Normalized fluorescence intensity as a function of pH for the Cy5.5-labelled NPs of PDPA80. TEM images of the siRNA-loaded NPs of PDPA80 at a pH of C) 6.5 and D) 6.0. E) In vitro siRNA release from the NPs of PDPA80 at 37 °C. F) Western blot analysis of surviving expression in the PC3 tumor tissue after systemic treatment by control NPs and anti-surviving siRNA-loaded NPs. G) Relative tumor size of the PC3 xenograft-tumor-bearing mice after treatment by PBS, control NPs, and anti-surviving siRNA-loaded NPs. The intravenous injections are indicated by the arrows. H) Representative image of the harvested PC3 tumor from each group at day 16. Anti-GL3 siRNA loaded NPs80 were used as a control. * P<0.05; ** P<0.01. Adapted with permission from Wiley Materials²¹³. All rights reserved 2016, Wiley Materials.

enhancing the endosomal escape efficiency²⁰⁹. In general, either the NPs alone or the NP-cargo conjugates can interact directly with the endosomal luminal membrane through charge-charge or hydrophobic interactions, leading to the local membrane destabilization and permeability. Studies have also shown that the CPPs mentioned above can also be used as an efficient endosomal escape motif^{210,211}. Trans-activating transcription (TAT)-peptide is one of the most thoroughly studied and extensively used CPPs for intracellular delivery. Dalal *et al.* developed a trans-activating transcription (TAT)-peptide-functionalized NP, which can direct their interactions with cells and increase the subcellular targeting efficiency as well²¹¹.

NPs that respond to select and specific stimuli provide another approach to enhance intracellular trafficking²¹². Xu *et al.* recently developed pH-responsive and tumor-penetrating nanoplatfoms for target siRNA delivery²¹³. The Cy5.5 labeled PDPA₈₀ showed low intensity at pH 6.5 due to the quenching of the aggregated fluorophores inside the hydrophobic cores of the self-assembled NPs, whereas the intensity increased significantly at pH 6.2 indicating the dissociation of the NPs. (Figure 10A-B) Therefore, this system showed the ability to respond to a very small pH range (In a range between 6.2 to 6.5). Intact NPs were also observed at pH 6.5 (Figure 10C) and NPs were dissociated at pH 6.2 through TEM (Figure 10D). In-vitro si-RNA release was also tested and showed a difference in release speed of the two pHs. Further in vitro and in vivo data both showed elongated blood circulation, and can efficiently target and penetrate the tumor parenchyma, resulting in efficient gene silencing and tumor growth inhibition (Shown in Figure 10F-H).

Certain organelles are associated with various diseases, but therapeutic molecules often fail to reach their subcellular target after being internalized by the cell. For instance, all DNA carriers must overcome the nuclear membrane to exert their function. Thus, recent research has focused on organelle targeting as a new vector for drug delivery. The nucleus is usually the final target of a therapeutic after crossing a series of biological barriers. Nuclear localization signals (NLS), for example, which are characterized by basic amino acids residues, have been widely used to functionalize NPs for the nuclear pore complex binding and cargo diffusing through the pores^{214,215}.

Mitochondria are power-generating organelles with bilayer membranes made mainly of protein, transforming oxygen and nutrients into adenosine triphosphate (ATP), and distributing energy throughout the cells. The dysfunction of mitochondria can cause a series of neurodegenerative diseases such as Parkinson's disease, or cancer^{216,217}. Therefore, mitochondrial targeting NPs have been developed to tackle the challenge. Similar to the NLS mentioned above, mitochondrial targeting signals (MTS) are characterized by 10-80 amino acids with amphiphilic structures²¹⁸. A recent

study conducted by Klimpel *et al.* combined the CPPs with MTS and developed a sequence with an amphipathic α -helical structure and high mitochondrial localization²¹⁹. Subcellular fraction results indicated that the conjugate was specifically accumulated inside the mitochondrial matrix. Other studies regarding the targeting approaches and penetration functionalization have been well summarized in other reviews^{212,214,218}.

4. Conclusions

In this review, we have described recent studies about peptide-based self-assembled nanostructures and their corresponding biomedical applications. Without any doubt, peptide-based nanostructures have grown exponentially over the past few decades owing to their bio-inspired properties, built simply by using a naturally generated building block: amino acids. The various amino acids possess distinct physical and chemical properties, such as charges, steric/conformational preferences, and functional groups, which affords huge potential functionalization possibilities and the intrinsic opportunity to arrange predictable structures based on secondary structures that the amino acids are capable of forming. The physicochemical versatility of the amino acids also enables the design of stimuli-responsive peptide motifs based on those in naturally occurring proteins or those designed *de novo*. As summarized above, peptides and/or proteins have also been used widely to encapsulate therapeutic cargos for target delivery including solubilization of poorly soluble drug molecules, improved drug pharmacokinetics and tissue distribution, enhanced targetability, improved antitumor efficacy, and reduced toxicity of drug molecules. And they can also be used to functionalize certain NPs to penetrate certain cell membranes or physical barriers including BBB.

However, despite the numerous advantages of the peptide-based NPs, only two protein-based NPs have been approved for use by the United States FDA¹⁶⁸. Despite the automated options for making highly pure peptides, most peptides have been created as a therapeutic cargo instead of a carrier because of the relatively high cost of production. Despite preclinical studies that demonstrate that most peptide-based NP show high cytocompatibility, additional large-scale investigations of their general immune safety are necessary. Further advances in evaluating the potential hazards in clinical trials and decreasing the cost of making peptides for large-scale applications will help advance these highly versatile carriers and treatment approaches into the clinic. It is worth mentioning that the complex formation of the peptide NPs can make predicting the behavior of those NPs challenging. Despite some molecular dynamic simulation work that has been conducted on those NPs, more versatile simulation models need to be addressed and with the help of the machine learning technics, further models that can more faithfully predict structure and function are foreseeable.

Acknowledgements

Related work in the Authors' laboratories was funded in part by the National Institutes of Health (R21 AR069778A, RO1 AR067247, 1 P30 GM110758, and both 1 P30 GM103519 and 1 P20 GM104316 for instrument resources) and in part by the National Science Foundation (BME 1605130, CBET 1703402, CBET 2023668). The contents of this manuscript do not necessarily reflect the views of the funding agencies.

References

1. Yadav, S., Sharma, A. K. & Kumar, P. Nanoscale Self-Assembly for Therapeutic Delivery. *Front. Bioeng. Biotechnol.* **8**, (2020).
2. Fallas, J. A., Leary, L. E. R. O. & Hartgerink, J. D. Synthetic collagen mimics: self-assembly of homotrimers, heterotrimers and higher order structures. *Chem. Soc. Rev.* **39**, 3510–3527 (2010).
3. Silver, F. H., Freeman, J. W. & Sehra, G. P. Collagen self-assembly and the development of tendon mechanical properties. *J. Biomech.* **36**, 1529–1553 (2003).
4. Luo, J. & Tong, Y. W. Self-assembly of collagen-mimetic peptide amphiphiles into biofunctional nanofiber. *ACS Nano* **5**, 7739–7747 (2011).
5. Wang, J. C. Moving one DNA double helix through another by a type II DNA topoisomerase: the story of a simple molecular machine. *Q. Rev. Biophys.* **31**, 107–144 (1998).
6. Róg, T., Pasenkiewicz-Gierula, M., Vattulainen, I. & Karttunen, M. Ordering effects of cholesterol and its analogues. *Biochim. Biophys. Acta - Biomembr.* **1788**, 97–121 (2009).
7. Zalba, S. & ten Hagen, T. L. M. Cell membrane modulation as adjuvant in cancer therapy. *Cancer Treat. Rev.* **52**, 48–57 (2017).
8. Jingya, Q., D., S. J. & L., K. K. Fine structural tuning of the assembly of ECM peptide conjugates via slight sequence modifications. *Sci. Adv.* **6**, eabd3033 (2022).
9. Luo, T. & Kiick, K. L. Noncovalent Modulation of the Inverse Temperature Transition and Self-Assembly of Elastin-b-Collagen-like Peptide Bioconjugates. *J. Am. Chem. Soc.* (2015) doi:10.1021/jacs.5b09941.
10. Koga, T., Kingetsu, S. & Higashi, N. Supramolecular Nanofibers from Collagen-Mimetic Peptides Bearing Various Aromatic Groups at N-Termini via Hierarchical Self-Assembly. *Int. J. Mol. Sci.* **2021**, Vol. 22, Page 4533 **22**, 4533 (2021).
11. Gnanasekaran, K. *et al.* Dipeptide Nanostructure Assembly and Dynamics via in Situ Liquid-Phase Electron Microscopy. *ACS Nano* **15**, 16542–16551 (2021).
12. Song, S. *et al.* Peptide interdigitation-induced twisted nanoribbons as chiral scaffolds for supramolecular nanozymes. *Nanoscale* **12**, 2422–2433 (2020).
13. Fan, Z. *et al.* Near infrared fluorescent peptide nanoparticles for enhancing esophageal cancer therapeutic efficacy. *Nat. Commun.* **2018 91 9**, 1–11 (2018).
14. Xie, J. *et al.* Cell-Penetrating Peptides in Diagnosis and Treatment of Human Diseases: From Preclinical Research to Clinical Application. *Front. Pharmacol.* **11**, 697 (2020).
15. Li, L., Xie, L., Zheng, R. & Sun, R. Self-Assembly Dipeptide Hydrogel: The Structures and Properties. *Front. Chem.* **9**, (2021).
16. Wang, B., Patkar, S. S. & Kiick, K. L. Application of Thermoresponsive Intrinsically Disordered Protein Polymers in Nanostructured and Microstructured Materials. *Macromol. Biosci.* **21**, 2100129 (2021).
17. Whitesides, G. M. & Grzybowski, B. Self-assembly at all scales. *Science (80-.)*. **295**, 2418–2421 (2002).
18. Kypr, J., Kejnovská, I., Renciuk, D. & Vorlíčková, M. Circular dichroism and conformational polymorphism of DNA. *Nucleic Acids Res.* **37**, 1713–1725 (2009).
19. Kabsch, W. & Sander, C. Dictionary of protein secondary structure: Pattern recognition of hydrogen-bonded and geometrical features. *Biopolymers* **22**, 2577–2637 (1983).
20. Wang, M., Huang, H., Zhang, Z. & Xiao, S. J. 2D DNA lattices constructed from two-tile DAE-O systems possessing circular central strands. *Nanoscale* **8**, 18870–18875 (2016).
21. Winfree, E., Liu, F., Wenzler, L. A. & Seeman, N. C. Design and self-assembly of two-dimensional DNA crystals. *Nat.* **1998 3946693 394**, 539–544 (1998).
22. Wei, B., Dai, M. & Yin, P. Complex shapes self-assembled from single-stranded DNA tiles. *Nature* **485**, 623–626 (2012).
23. Schnaider, L. *et al.* Self-assembling dipeptide antibacterial nanostructures with membrane disrupting activity. *Nat. Commun.* **2017 81 8**, 1–10 (2017).
24. Caiaffa, K. S. *et al.* Cytocompatibility and Synergy of EGCG and Cationic Peptides Against Bacteria Related to Endodontic Infections, in Planktonic and Biofilm Conditions. *Probiotics Antimicrob. Proteins* **13**, 1808–1819 (2021).
25. Reja, A., Afrose, S. P. & Das, D. Aldolase Cascade Facilitated by Self-Assembled Nanotubes from Short Peptide Amphiphiles. *Angew. Chemie Int. Ed.* **59**, 4329–4334 (2020).
26. Liu, S., Du, P., Sun, H., Yu, H. Y. & Wang, Z. G. Bioinspired supramolecular catalysts from designed self-assembly of DNA or peptides. *ACS Catal.* **10**, 14937–14958 (2020).
27. Wang, C. *et al.* Enantioselective Diels–Alder Reactions with G-Quadruplex DNA-Based Catalysts. *Angew. Chemie Int. Ed.* **51**, 9352–9355 (2012).
28. Hwang, J. *et al.* In Situ Imaging of Tissue Remodeling with Collagen Hybridizing Peptides. *ACS Nano* **11**, 9825–9835 (2017).

29. Désogère, P., Montesi, S. B. & Caravan, P. Molecular Probes for Imaging Fibrosis and Fibrogenesis. *Chem. – A Eur. J.* **25**, 1128–1141 (2019).
30. Vert, M. *et al.* Terminology for biorelated polymers and applications (IUPAC recommendations 2012). *Pure Appl. Chem.* **84**, 377–410 (2012).
31. Baroli, B. *et al.* Penetration of Metallic Nanoparticles in Human Full-Thickness Skin. *J. Invest. Dermatol.* **127**, 1701–1712 (2007).
32. Brown, T. D., Habibi, N., Wu, D., Lahann, J. & Mitragotri, S. Effect of Nanoparticle Composition, Size, Shape, and Stiffness on Penetration across the Blood-Brain Barrier. *ACS Biomater. Sci. Eng.* **6**, 4916–4928 (2020).
33. Blanco, E., Shen, H. & Ferrari, M. Principles of nanoparticle design for overcoming biological barriers to drug delivery. *Nat. Biotechnol.* **33**, 941 (2015).
34. Yang, G. *et al.* Bioinspired Core–Shell Nanoparticles for Hydrophobic Drug Delivery. *Angew. Chemie* **131**, 14495–14502 (2019).
35. Kalepu, S. & Nekkanti, V. Insoluble drug delivery strategies: review of recent advances and business prospects. *Acta Pharm. Sin. B* **5**, 442–453 (2015).
36. Duncan, B., Kim, C. & Rotello, V. M. Gold nanoparticle platforms as drug and biomacromolecule delivery systems. *J. Control. Release* **148**, 122–127 (2010).
37. Bhattacharyya, J. *et al.* A paclitaxel-loaded recombinant polypeptide nanoparticle outperforms Abraxane in multiple murine cancer models. *Nat. Commun.* **2015** *6*, 1–12 (2015).
38. Zielinska, A. *et al.* Polymeric Nanoparticles: Production, Characterization, Toxicology and Ecotoxicology. *Molecules* **25**, (2020).
39. Cano, A. *et al.* Dual-drug loaded nanoparticles of Epigallocatechin-3-gallate (EGCG)/Ascorbic acid enhance therapeutic efficacy of EGCG in a APPsw/PS1dE9 Alzheimer’s disease mice model. *J. Control. Release* **301**, 62–75 (2019).
40. Bratek-Skicki, A. Towards a new class of stimuli-responsive polymer-based materials – Recent advances and challenges. *Appl. Surf. Sci. Adv.* **4**, 100068 (2021).
41. Palanikumar, L. *et al.* pH-responsive high stability polymeric nanoparticles for targeted delivery of anticancer therapeutics. *Commun. Biol.* **3**, (2020).
42. Zhang, Z. *et al.* Brightness Enhancement of Near-Infrared Semiconducting Polymer Dots for in Vivo Whole-Body Cell Tracking in Deep Organs. *ACS Appl. Mater. Interfaces* **10**, 26928–26935 (2018).
43. Calzoni, E. *et al.* Biocompatible Polymer Nanoparticles for Drug Delivery Applications in Cancer and Neurodegenerative Disorder Therapies. *J. Funct. Biomater.* **10**, (2019).
44. Kapadia, C. H., Ioele, S. A. & Day, E. S. Layer-by-layer assembled PLGA nanoparticles carrying miR-34a cargo inhibit the proliferation and cell cycle progression of triple-negative breast cancer cells. *J. Biomed. Mater. Res. Part A* **108**, 601–613 (2020).
45. Harris, J. C., Scully, M. A. & Day, E. S. Cancer Cell Membrane-Coated Nanoparticles for Cancer Management. *Cancers* **2019**, Vol. 11, Page 1836 **11**, 1836 (2019).
46. Valcourt, D. M., Dang, M. N. & Day, E. S. IR820-loaded PLGA nanoparticles for photothermal therapy of triple-negative breast cancer. *J. Biomed. Mater. Res. Part A* **107**, 1702–1712 (2019).
47. Danhier, F. *et al.* PLGA-based nanoparticles: An overview of biomedical applications. *J. Control. Release* **161**, 505–522 (2012).
48. Papoutsakis, E. T. *et al.* Biomembrane-covered nanoparticles (bionps) for delivering active agents to stem cells. (2021).
49. Kao, C. Y. & Papoutsakis, E. T. Engineering human megakaryocytic microparticles for targeted delivery of nucleic acids to hematopoietic stem and progenitor cells. *Sci. Adv.* **4**, (2018).
50. Jiang, J., Kao, C. Y. & Papoutsakis, E. T. How do megakaryocytic microparticles target and deliver cargo to alter the fate of hematopoietic stem cells? *J. Control. Release* **247**, 1–18 (2017).
51. Fay, B. L., Melamed, J. R. & Day, E. S. Nanoshell-mediated photothermal therapy can enhance chemotherapy in inflammatory breast cancer cells. *Int. J. Nanomedicine* **10**, 6931 (2015).
52. Li, D. *et al.* Influence of Particle Geometry on Gastrointestinal Transit and Absorption following Oral Administration. *ACS Appl. Mater. Interfaces* **9**, 42492–42502 (2017).
53. Silva, A. M. *et al.* In Vitro Cytotoxicity of Oleanolic/Ursolic Acids-Loaded in PLGA Nanoparticles in Different Cell Lines. *Pharmaceutics* **11**, (2019).
54. Lombardo, D., Kiselev, M. A. & Caccamo, M. T. Smart Nanoparticles for Drug Delivery Application: Development of Versatile Nanocarrier Platforms in Biotechnology and Nanomedicine. *J. Nanomater.* **2019**, (2019).
55. Akbarzadeh, A. *et al.* Liposome: classification, preparation, and applications. *Nanoscale Res. Lett.* **8**, 102 (2013).
56. Gonda, A. *et al.* Engineering Tumor-Targeting Nanoparticles as Vehicles for Precision Nanomedicine. *Med One* **4**, e190021 (2019).
57. Sercombe, L. *et al.* Advances and challenges of liposome assisted drug delivery. *Frontiers in Pharmacology* (2015) doi:10.3389/fphar.2015.00286.
58. Merrifield R B. Synthesis of a Tetrapeptide. *J. Am. Chem. Soc.* **85**, 2149–2154 (1963).
59. Kuliopulos, A. & Walsh, C. T. Production, Purification, and Cleavage of Tandem Repeats of Recombinant Peptides. *J. Am. Chem. Soc.* **116**, 4599–4607 (1994).

60. Chen, W. *et al.* Self-Assembled Peptide Nanofibers Display Natural Antimicrobial Peptides to Selectively Kill Bacteria without Compromising Cytocompatibility. *ACS Appl. Mater. Interfaces* **11**, 28681–28689 (2019).
61. D'souza, A. *et al.* Nine-Residue Peptide Self-Assembles in the Presence of Silver to Produce a Self-Healing, Cytocompatible, Antimicrobial Hydrogel. *ACS Appl. Mater. Interfaces* **12**, 17091–17099 (2020).
62. Matson, J. B., Zha, R. H. & Stupp, S. I. Peptide Self-Assembly for Crafting Functional Biological Materials. *Curr. Opin. Solid State Mater. Sci.* **15**, 225 (2011).
63. Egli, J., Siebler, C., Köhler, M., Zenobi, R. & Wennemers, H. Hydrophobic Moieties Bestow Fast-Folding and Hyperstability on Collagen Triple Helices. *J. Am. Chem. Soc.* **141**, 5607–5611 (2019).
64. Singh, A. K. Structure, Synthesis, and Application of Nanoparticles. *Eng. Nanoparticles* 19–76 (2016) doi:10.1016/B978-0-12-801406-6.00002-9.
65. Mohan, T., Kleinschek, K. S. & Kargl, R. Polysaccharide peptide conjugates: Chemistry, properties and applications. *Carbohydr. Polym.* **280**, 118875 (2022).
66. Jeong, W. jin *et al.* Peptide–nanoparticle conjugates: a next generation of diagnostic and therapeutic platforms? *Nano Converg. 2018 51* **5**, 1–18 (2018).
67. Tarvirdipour, S., Huang, X., Mihali, V., Schoenenberger, C. A. & Palivan, C. G. Peptide-Based Nanoassemblies in Gene Therapy and Diagnosis: Paving the Way for Clinical Application. *Molecules* **25**, (2020).
68. Thapa, R. K. & Sullivan, M. O. Gene delivery by peptide-assisted transport. *Curr. Opin. Biomed. Eng.* **7**, 71 (2018).
69. Ngo, H. X. & Garneau-Tsodikova, S. What are the drugs of the future? *Medchemcomm* **9**, 757–758 (2018).
70. Zhai, Z. *et al.* Erythrocyte-mimicking paclitaxel nanoparticles for improving biodistributions of hydrophobic drugs to enhance antitumor efficacy. *Drug Deliv.* **27**, 387–399 (2020).
71. Polderman, J. A. *et al.* Adverse side effects of dexamethasone in surgical patients. *Cochrane Database Syst. Rev.* **2019**, (2018).
72. Hanafy, N. A. N., El-Kemary, M. & Leporatti, S. Micelles Structure Development as a Strategy to Improve Smart Cancer Therapy. *Cancers 2018, Vol. 10, Page 238* **10**, 238 (2018).
73. Fernández-Carneado, J., Kogan, M. J., Pujals, S. & Giralt, E. Amphipathic peptides and drug delivery. *Pept. Sci.* **76**, 196–203 (2004).
74. Sis, M. J. & Webber, M. J. Drug Delivery with Designed Peptide Assemblies. *Trends Pharmacol. Sci.* **40**, 747–762 (2019).
75. Ruan, L., Chen, W., Wang, R., Lu, J. & Zink, J. I. Magnetically Stimulated Drug Release Using Nanoparticles Capped by Self-Assembling Peptides. *ACS Appl. Mater. Interfaces* **11**, 43835–43842 (2019).
76. Luo, T. *et al.* Thermoresponsive Elastin-b-Collagen-Like Peptide Bioconjugate Nanovesicles for Targeted Drug Delivery to Collagen-Containing Matrices. *Biomacromolecules* (2017) doi:10.1021/acs.biomac.7b00686.
77. Islam, Y. *et al.* Peptide based drug delivery systems to the brain. *Nano Express* **1**, 012002 (2020).
78. Sousa De Almeida, M. *et al.* Understanding nanoparticle endocytosis to improve targeting strategies in nanomedicine. *Chem. Soc. Rev.* **50**, 5397–5434 (2021).
79. Gagliardi, A. *et al.* Biodegradable Polymeric Nanoparticles for Drug Delivery to Solid Tumors. *Front. Pharmacol.* **12**, 17 (2021).
80. Kamaly, N., Yameen, B., Wu, J. & Farokhzad, O. C. Degradable controlled-release polymers and polymeric nanoparticles: Mechanisms of controlling drug release. *Chem. Rev.* **116**, 2602–2663 (2016).
81. Mitchell, M. J. *et al.* Engineering precision nanoparticles for drug delivery. *Nat. Rev. Drug Discov. 2020 202* **20**, 101–124 (2020).
82. Yaqoob, A. A. *et al.* Recent Advances in Metal Decorated Nanomaterials and Their Various Biological Applications: A Review. *Front. Chem.* **8**, 341 (2020).
83. Andleeb, A. *et al.* A Systematic Review of Biosynthesized Metallic Nanoparticles as a Promising Anti-Cancer-Strategy. *Cancers 2021, Vol. 13, Page 2818* **13**, 2818 (2021).
84. Chandrakala, V., Aruna, V. & Angajala, G. Review on metal nanoparticles as nanocarriers: current challenges and perspectives in drug delivery systems. *Emergent Mater.* **1**, 1–23 (2022).
85. Spireanu, V. A., Chircov, C., Grumezescu, A. M., Vasile, B. Ştefan & Andronescu, E. Inorganic Nanoparticles and Composite Films for Antimicrobial Therapies. *Int. J. Mol. Sci. 2021, Vol. 22, Page 4595* **22**, 4595 (2021).
86. Liu, X., Wu, Z., Cavalli, R. & Cravotto, G. Sonochemical Preparation of Inorganic Nanoparticles and Nanocomposites for Drug Release-A Review. *Ind. Eng. Chem. Res.* **60**, 10011–10032 (2021).
87. Avellan, A. *et al.* Critical Review: Role of Inorganic Nanoparticle Properties on Their Foliar Uptake and in Planta Translocation. *Environ. Sci. Technol.* **55**, 13417–13431 (2021).
88. Egli, M. & Zhang, S. How the α -helix got its name. *Nat. Rev. Mol. Cell Biol.* **2022 233** **23**, 165–165 (2022).
89. Magnotti, E. L. *et al.* Self-Assembly of an α -Helical Peptide into a Crystalline Two-Dimensional Nanoporous Framework. *J. Am. Chem. Soc.* **138**, 16274–16282 (2016).
90. Bera, S. & Gazit, E. Self-assembly of Functional

- Nanostructures by Short Helical Peptide Building Blocks. **26**,.
91. Wang, F. *et al.* Structural analysis of cross α -helical nanotubes provides insight into the designability of filamentous peptide nanomaterials. *Nat. Commun.* **2021** *12* **1**, 1–14 (2021).
92. Beesley, J. L. & Woolfson, D. N. The de novo design of α -helical peptides for supramolecular self-assembly. *Curr. Opin. Biotechnol.* **58**, 175–182 (2019).
93. Hughes, S. A. *et al.* Ambidextrous helical nanotubes from self-assembly of designed helical hairpin motifs. *Proc. Natl. Acad. Sci. U. S. A.* **116**, 14456–14464 (2019).
94. Kumar, P. & Bansal, M. Dissecting π -helices: Sequence, structure and function. *FEBS J.* **282**, 4415–4432 (2015).
95. Truebestein, L. & Leonard, T. A. Coiled-coils: The long and short of it. *Bioessays* **38**, 903 (2016).
96. Fletcher, J. M. *et al.* Self-assembling cages from coiled-coil peptide modules. *Science (80-.)*. **340**, 595–599 (2013).
97. Utterström, J., Naeimipour, S., Selegård, R. & Aili, D. Coiled coil-based therapeutics and drug delivery systems. *Adv. Drug Deliv. Rev.* **170**, 26–43 (2021).
98. Lapenta, F., Aupič, J., Strmšek, Ž. & Jerala, R. Coiled coil protein origami: from modular design principles towards biotechnological applications. *Chem. Soc. Rev.* **47**, 3530–3542 (2018).
99. Buchberger, A., Simmons, C. R., Fahmi, N. E., Freeman, R. & Stephanopoulos, N. Hierarchical Assembly of Nucleic Acid/Coiled-Coil Peptide Nanostructures. *J. Am. Chem. Soc.* **142**, 1406–1416 (2020).
100. Ludwiczak, J., Winski, A., Szczepaniak, K., Alva, V. & Dunin-Horkawicz, S. DeepCoil—a fast and accurate prediction of coiled-coil domains in protein sequences. *Bioinformatics* **35**, 2790–2795 (2019).
101. Liu, J. *et al.* A seven-helix coiled coil. *Proc. Natl. Acad. Sci.* **103**, 15457–15462 (2006).
102. Nishiyama, T., Sugiura, K., Sugikawa, K., Ikeda, A. & Mizuno, T. Construction of protein-loadable protein cages using the hybrid proteins of the oleosin hydrophobic domain and hydrophilic dimeric coiled-coil. *Colloid Interface Sci. Commun.* **40**, 100352 (2021).
103. Rawlings, A. E. *et al.* Artificial coiled coil biomineralisation protein for the synthesis of magnetic nanoparticles. *Nat. Commun.* **2019** *10* **10**, 1–9 (2019).
104. Tunn, I., Harrington, M. J. & Blank, K. G. Bioinspired Histidine⁻Zn(2+) Coordination for Tuning the Mechanical Properties of Self-Healing Coiled Coil Cross-Linked Hydrogels. *Biomimetics (Basel, Switzerland)* **4**, 25 (2019).
105. Barnes, B. E. *et al.* Synthesis and Characterization of a Leucine-Based Block Co-Polypeptide: The Effect of the Leucine Zipper on Self-Assembly. *Biomacromolecules* **21**, 2463–2472 (2020).
106. Xiong, Q., Stupp, S. I. & Schatz, G. C. Molecular Insight into the β -Sheet Twist and Related Morphology of Self-Assembled Peptide Amphiphile Ribbons. *J. Phys. Chem. Lett.* **12**, 11238–11244 (2021).
107. Kuczera, S., Rüter, A., Roger, K. & Olsson, U. Two Dimensional Oblique Molecular Packing within a Model Peptide Ribbon Aggregate. *ChemPhysChem* **21**, 1519–1523 (2020).
108. Ma, X. *et al.* Ordered Packing of β -Sheet Nanofibrils into Nanotubes: Multi-hierarchical Assembly of Designed Short. *Nano Lett.* **21**, 10199–10207 (2021).
109. Wang, F. *et al.* Deterministic chaos in the self-assembly of β sheet nanotubes from an amphipathic oligopeptide. *Matter* **4**, 3217–3231 (2021).
110. Ashkenasy, N., Horne, W. S. & Ghadiri, M. R. Design of self-assembling peptide nanotubes with delocalized electronic states. *Small* **2**, 99–102 (2006).
111. Ping, Y. *et al.* Supramolecular β -Sheets Stabilized Protein Nanocarriers for Drug Delivery and Gene Transfection. *ACS Nano* **11**, 4528–4541 (2017).
112. Reeb, J. & Rost, B. Secondary Structure Prediction. *Encycl. Bioinforma. Comput. Biol. ABC Bioinforma.* **1–3**, 488–496 (2019).
113. Perutz, M. F., Staden, R., Moens, L. & De Baere, I. Polar zippers. *Curr. Biol.* **3**, 249–253 (1993).
114. Wang, M. *et al.* Nanoribbons self-assembled from short peptides demonstrate the formation of polar zippers between β -sheets. *Nat. Commun.* **9**, 5118 (2018).
115. Ding, D. *et al.* Squid suckerin microneedle arrays for tunable drug release. *J. Mater. Chem. B* **5**, 8467–8478 (2017).
116. Hiew, S. H. & Miserez, A. Squid Sucker Ring Teeth: Multiscale Structure–Property Relationships, Sequencing, and Protein Engineering of a Thermoplastic Biopolymer. *ACS Biomater. Sci. Eng.* **3**, 680–693 (2017).
117. Wang, M. *et al.* Left or Right: How Does Amino Acid Chirality Affect the Handedness of Nanostructures Self-Assembled from Short Amphiphilic Peptides? *J. Am. Chem. Soc.* **139**, 4185–4194 (2017).
118. Chen, J. & Zou, X. Self-assemble peptide biomaterials and their biomedical applications. *Bioact. Mater.* **4**, 120–131 (2019).
119. Sinha, N. J., Langenstein, M. G., Pochan, D. J., Kloxin, C. J. & Saven, J. G. Peptide Design and Self-assembly into Targeted Nanostructure and Functional Materials. *Chem. Rev.* **121**, 13915–13935 (2021).
120. Luo, T. & Kiick, K. L. Collagen-Like Peptide Bioconjugates. *Bioconjugate Chemistry* (2017) doi:10.1021/acs.bioconjchem.6b00673.
121. Li, Y. *et al.* Targeting collagen strands by photo-triggered triple-helix hybridization. *Proc. Natl. Acad. Sci. U. S. A.* (2012) doi:10.1073/pnas.1209721109.
122. O’Leary, L. E. R. R., Fallas, J. A., Bakota, E. L.,

- Kang, M. K. & Hartgerink, J. D. Multi-hierarchical self-assembly of a collagen mimetic peptide from triple helix to nanofibre and hydrogel. *Chem.* **3**, 821–828 (2011).
123. Lee, H. J. *et al.* Collagen mimetic peptide-conjugated photopolymerizable PEG hydrogel. *Biomaterials* **27**, 5268–5276 (2006).
124. Chatterjee, S. & Hui, P. C. L. Review of Applications and Future Prospects of Stimuli-Responsive Hydrogel Based on Thermo-Responsive Biopolymers in Drug Delivery Systems. *Polym. 2021, Vol. 13, Page 2086* **13**, 2086 (2021).
125. San, B. H. *et al.* Self-Assembled Water-Soluble Nanofibers Displaying Collagen Hybridizing Peptides. *J. Am. Chem. Soc.* **139**, 16640–16649 (2017).
126. Zitnay, J. L. *et al.* Accumulation of collagen molecular unfolding is the mechanism of cyclic fatigue damage and failure in collagenous tissues. *Sci. Adv.* **6**, 2795 (2020).
127. Chen, Y. *et al.* Targeted pathological collagen delivery of sustained-release rapamycin to prevent heterotopic ossification. *Sci. Adv.* **6**, (2020).
128. Kessler, J. L. *et al.* Peptoid Residues Make Diverse, Hyperstable Collagen Triple-Helices. *J. Am. Chem. Soc.* **143**, 10910–10919 (2021).
129. Zhang, R. *et al.* Peptide Amphiphile Micelle Vaccine Size and Charge Influence the Host Antibody Response. *ACS Biomater. Sci. Eng.* **4**, 2463–2472 (2018).
130. Zhang, R. *et al.* Instructive Design of Triblock Peptide Amphiphiles for Structurally Complex Micelle Fabrication. *ACS Biomater. Sci. Eng.* **4**, 2330–2339 (2018).
131. Rahman, M. M., Ueda, M., Hirose, T. & Ito, Y. Spontaneous Formation of Gating Lipid Domain in Uniform-Size Peptide Vesicles for Controlled Release. *J. Am. Chem. Soc.* **140**, 17956–17961 (2018).
132. Tsonchev, S., Niece, K. L., Schatz, G. C., Ratner, M. A. & Stupp, S. I. Phase Diagram for Assembly of Biologically-Active Peptide Amphiphiles†. *J. Phys. Chem. B* **112**, 441–447 (2007).
133. Hendricks, M. P., Sato, K., Palmer, L. C. & Stupp, S. I. Supramolecular Assembly of Peptide Amphiphiles. *Acc. Chem. Res.* **50**, 2440–2448 (2017).
134. Zhu, H. *et al.* Supramolecular peptide constructed by molecular Lego allowing programmable self-assembly for photodynamic therapy. *Nat. Commun.* **10**, 2412 (2019).
135. Fry, H. C., Peters, B. L. & Ferguson, A. L. Pushing and Pulling: A Dual pH Trigger Controlled by Varying the Alkyl Tail Length in Heme Coordinating Peptide Amphiphiles. *J. Phys. Chem. B* **125**, 1317–1330 (2021).
136. Dong, W. *et al.* Antimicrobial activity and self-assembly behavior of antimicrobial peptide chensinin-1b with lipophilic alkyl tails. *Eur. J. Med. Chem.* **150**, 546–558 (2018).
137. Yaguchi, A. *et al.* Hydrogel-Stiffening and Non-Cell Adhesive Properties of Amphiphilic Peptides with Central Alkylene Chains. *Chem. – A Eur. J.* **27**, 9295–9301 (2021).
138. Taylor, P. A., Huang, H., Kiick, K. L. & Jayaraman, A. Placement of tyrosine residues as a design element for tuning the phase transition of elastin-peptide-containing conjugates: experiments and simulations. *Mol. Syst. Des. Eng.* **5**, 1239–1254 (2020).
139. Dunshee, L. C., Sullivan, M. O. & Kiick, K. L. Manipulation of the dually thermoresponsive behavior of peptide-based vesicles through modification of collagen-like peptide domains. *Bioeng. Transl. Med.* (2020) doi:10.1002/btm2.10145.
140. Lombardo, D., Kiselev, M. A., Magazù, S. & Calandra, P. Amphiphiles self-assembly: Basic concepts and future perspectives of supramolecular approaches. *Adv. Condens. Matter Phys.* **2015**, (2015).
141. Parshad, B. *et al.* Non-ionic small amphiphile based nanostructures for biomedical applications. *RSC Adv.* **10**, 42098–42115 (2020).
142. Singh, A. K. *et al.* Aggregation Behavior of Non-ionic Twinned Amphiphiles and Their Application as Biomedical Nanocarriers. *Chem. – An Asian J.* **12**, 1796–1806 (2017).
143. Panda, J. J. & Chauhan, V. S. Short peptide based self-assembled nanostructures: implications in drug delivery and tissue engineering. *Polym. Chem.* **5**, 4418–4436 (2014).
144. Tenidis, K. *et al.* Identification of a penta- and hexapeptide of islet amyloid polypeptide (IAPP) with amyloidogenic and cytotoxic properties. *J. Mol. Biol.* **295**, 1055–1071 (2000).
145. Adler-Abramovich, L. *et al.* Phenylalanine assembly into toxic fibrils suggests amyloid etiology in phenylketonuria. *Nat. Chem. Biol.* **2012** **8**, 701–706 (2012).
146. Yang, Z. *et al.* Enzymatic Formation of Supramolecular Hydrogels. *Adv. Mater.* **16**, 1440–1444 (2004).
147. Nelli, S. R., Chakravarthy, R. D., Xing, Y.-M., Weng, J.-P. & Lin, H.-C. Self-assembly of single amino acid/pyrene conjugates with unique structure–morphology relationship. *Soft Matter* **13**, 8402–8407 (2017).
148. Han, S. *et al.* Self-Assembly of Short Peptide Amphiphiles: The Cooperative Effect of Hydrophobic Interaction and Hydrogen Bonding. *Chem. – A Eur. J.* **17**, 13095–13102 (2011).
149. Zhao, Y. *et al.* Tuning One-Dimensional Nanostructures of Bola-Like Peptide Amphiphiles by Varying the Hydrophilic Amino Acids. *Chem. – A Eur. J.* **22**, 11394–11404 (2016).
150. Glossop, H. D. *et al.* Battacin-Inspired Ultrashort

- 1
2
3 Peptides: Nanostructure Analysis and Antimicrobial Activity. *Biomacromolecules* **20**, 2515–2529 (2019).
- 4 151. Ayala, L. *et al.* Polymeric peptide pigments with
5 sequence-encoded properties. *Science (80-.)*. **356**,
6 1064–1068 (2017).
- 7 152. Hu, X. *et al.* Recent advances in short peptide self-
8 assembly: from rational design to novel applications.
9 *Curr. Opin. Colloid Interface Sci.* **45**, 1–13 (2020).
- 10 153. Reches, M. & Gazit, E. Casting metal nanowires
11 within discrete self-assembled peptide nanotubes.
12 *Science (80-.)*. **300**, 625–627 (2003).
- 13 154. Chibh, S., Mishra, J., Kour, A., Chauhan, V. S. &
14 Panda, J. J. Recent advances in the fabrication and
15 bio-medical applications of self-assembled dipeptide
16 nanostructures. [https://doi.org/10.2217/nmm-2020-](https://doi.org/10.2217/nmm-2020-0314)
17 *0314* **16**, 139–163 (2021).
- 18 155. Shintani, Y. *et al.* Formation of supramolecular
19 nanostructures via in situ self-assembly and post-
20 assembly modification of a biocatalytically
21 constructed dipeptide hydrazide. (2021)
22 doi:10.26434/CHEMRXIV-2021-45RKS.
- 23 156. Li, Q., Li, X. & Zhao, C. Strategies to Obtain
24 Encapsulation and Controlled Release of Small
25 Hydrophilic Molecules. *Front. Bioeng. Biotechnol.* **8**,
26 437 (2020).
- 27 157. Che, H. & van Hest, J. C. M. Adaptive Polymersome
28 Nanoreactors. *ChemNanoMat* **5**, 1092–1109 (2019).
- 29 158. Veloso, S. R. S., Andrade, R. G. D. & Castanheira,
30 E. M. S. Review on the advancements of magnetic
31 gels: towards multifunctional magnetic liposome-
32 hydrogel composites for biomedical applications.
33 *Adv. Colloid Interface Sci.* **288**, 102351 (2021).
- 34 159. Daraee, H., Etemadi, A., Kouhi, M., Alimirzalu, S. &
35 Akbarzadeh, A. Application of liposomes in
36 medicine and drug delivery.
37 <https://doi.org/10.3109/21691401.2014.953633> **44**,
38 381–391 (2014).
- 39 160. Yuan, L. & Liu, L. Peptide-based electrochemical
40 biosensing. *Sensors Actuators B Chem.* **344**, 130232
41 (2021).
- 42 161. Negahdary, M. & Heli, H. An electrochemical
43 peptide-based biosensor for the Alzheimer biomarker
44 amyloid- β (1–42) using a microporous gold
45 nanostructure. *Microchim. Acta* **186**, 1–8 (2019).
- 46 162. Liu, X., Sun, X. & Liang, G. Peptide-based
47 supramolecular hydrogels for bioimaging
48 applications. *Biomater. Sci.* **9**, 315–327 (2021).
- 49 163. Qi, G.-B. *et al.* Self-Assembled Peptide-Based
50 Nanomaterials for Biomedical Imaging and Therapy.
51 *Adv. Mater.* **30**, 1703444 (2018).
- 52 164. Kadonosono, T. *et al.* Cell penetrating peptides
53 improve tumor delivery of cargos through
54 neuropilin-1-dependent extravasation. *J. Control.*
55 *Release* **201**, 14–21 (2015).
- 56 165. Tian, Y. *et al.* Integration of Cell-Penetrating
57 Peptides with Rod-like Bionanoparticles: Virus-
58 Inspired Gene-Silencing Technology. *Nano Lett.* **18**,
59 5453–5460 (2018).
- 60 166. Pescina, S. *et al.* Cell penetrating peptides in ocular
drug delivery: State of the art. *J. Control. Release*
284, 84–102 (2018).
167. King, W. *et al.* Risks of Precipitate Formation When
Combining Corticosteroids with Local Anesthetic for
Use During Interventional Pain Procedures. *Pain*
Med. **21**, 423–424 (2020).
168. Hong, S. *et al.* Protein-Based Nanoparticles as Drug
Delivery Systems. *Pharmaceutics* **12**, 1–28 (2020).
169. Wang, L. *et al.* Therapeutic peptides: current
applications and future directions. *Signal Transduct.*
Target. Ther. **2022** *71* **7**, 1–27 (2022).
170. Nalini, T., Basha, S. K., Mohamed Sadiq, A. M.,
Kumari, V. S. & Kaviyarasu, K. Development and
characterization of alginate / chitosan nanoparticulate
system for hydrophobic drug encapsulation. *J. Drug*
Deliv. Sci. Technol. **52**, 65–72 (2019).
171. Santos, A. C. *et al.* Halloysite clay nanotubes for life
sciences applications: From drug encapsulation to
bioscaffold. *Adv. Colloid Interface Sci.* **257**, 58–70
(2018).
172. Duro-Castano, A. *et al.* Designing peptide
nanoparticles for efficient brain delivery. *Adv. Drug*
Deliv. Rev. **160**, 52–77 (2020).
173. Tran, T. T. D. & Tran, P. H. L. Nanoconjugation and
Encapsulation Strategies for Improving Drug
Delivery and Therapeutic Efficacy of Poorly Water-
Soluble Drugs. *Pharmaceutics* **11**, (2019).
174. Shah, A. *et al.* Stimuli-responsive peptide-based
biomaterials as drug delivery systems. *Chem. Eng. J.*
353, 559–583 (2018).
175. Zegota, M. M. *et al.* Dual Stimuli-Responsive
Dynamic Covalent Peptide Tags: Toward Sequence-
Controlled Release in Tumor-like
Microenvironments. *J. Am. Chem. Soc.* **143**, 17047–
17058 (2021).
176. Zhang, X. *et al.* Dual Stimuli-Responsive Peptide-
Based Palladium Nano-Lychee Spheres for
Synergistic Antitumor Therapy. *ACS Biomater. Sci.*
Eng. **5**, 4474–4484 (2019).
177. Asati, S., Pandey, V. & Soni, V. RGD Peptide as a
Targeting Moiety for Theranostic Purpose: An
Update Study. *Int. J. Pept. Res. Ther.* **2018** *251* **25**,
49–65 (2018).
178. Hatley, R. J. D. *et al.* An α v-RGD Integrin Inhibitor
Toolbox: Drug Discovery Insight, Challenges and
Opportunities. *Angew. Chemie Int. Ed.* **57**, 3298–
3321 (2018).
179. Lovejoy, D. A. *et al.* Synthetic Peptides as
Therapeutic Agents: Lessons Learned From
Evolutionary Ancient Peptides and Their Transit
Across Blood-Brain Barriers. *Front. Endocrinol.*
(Lausanne). **10**, 730 (2019).
180. Yang, M. *et al.* Function and Mechanism of RGD in
Bone and Cartilage Tissue Engineering. *Front.*
Bioeng. Biotechnol. **9**, 1184 (2021).
181. Du, C. *et al.* Epidermal Growth Factor Receptor-
Targeting Peptide Nanoparticles Simultaneously

- 1
2
3 Deliver Gemcitabine and Olaparib To Treat
4 Pancreatic Cancer with Breast Cancer 2 (BRCA2)
5 Mutation. *ACS Nano* **12**, 10785–10796 (2018).
- 6 182. Moyer, T. J. *et al.* Self-Assembled Peptide
7 Nanostructures Targeting Death Receptor 5 and
8 Encapsulating Paclitaxel As a Multifunctional
9 Cancer Therapy. *ACS Biomater. Sci. Eng.* **5**, 6046–
10 6053 (2019).
- 11 183. Behzadi, S. *et al.* Cellular uptake of nanoparticles:
12 journey inside the cell. **46**, 4218–4244 (2017).
- 13 184. Ventola, C. L. Progress in Nanomedicine: Approved
14 and Investigational Nanodrugs. *Pharm. Ther.* **42**, 742
15 (2017).
- 16 185. Wang, S. H., Lee, C. W., Chiou, A. & Wei, P. K.
17 Size-dependent endocytosis of gold nanoparticles
18 studied by three-dimensional mapping of plasmonic
19 scattering images. *J. Nanobiotechnology* **8**, 1–13
20 (2010).
- 21 186. Foroozandeh, P. & Aziz, A. A. Insight into Cellular
22 Uptake and Intracellular Trafficking of
23 Nanoparticles. doi:10.1186/s11671-018-2728-6.
- 24 187. Ho, Y. T., Kamm, R. D. & Kah, J. C. Y. Influence of
25 protein corona and caveolae-mediated endocytosis on
26 nanoparticle uptake and transcytosis. *Nanoscale* **10**,
27 12386–12397 (2018).
- 28 188. Mosquera, J., García, I. & Liz-Marzán, L. M.
29 Cellular Uptake of Nanoparticles versus Small
30 Molecules: A Matter of Size. *Acc. Chem. Res.* **51**,
31 2305–2313 (2018).
- 32 189. Cheng, X. *et al.* Protein Corona Influences Cellular
33 Uptake of Gold Nanoparticles by Phagocytic and
34 Nonphagocytic Cells in a Size-Dependent Manner.
35 *ACS Appl. Mater. Interfaces* **7**, 20568–20575 (2015).
- 36 190. Arnida, Malugin, A. & Ghandehari, H. Cellular
37 uptake and toxicity of gold nanoparticles in prostate
38 cancer cells: a comparative study of rods and
39 spheres. *J. Appl. Toxicol.* **30**, 212–217 (2010).
- 40 191. Geng, Y. *et al.* Shape effects of filaments versus
41 spherical particles in flow and drug delivery. *Nat.*
42 *Nanotechnol.* **2**, 249–255 (2007).
- 43 192. Xie, X., Liao, J., Shao, X., Li, Q. & Lin, Y. The
44 Effect of shape on Cellular Uptake of Gold
45 Nanoparticles in the forms of Stars, Rods, and
46 Triangles. *Sci. Reports 2017 71* **7**, 1–9 (2017).
- 47 193. Banerjee, A., Qi, J., Gogoi, R., Wong, J. &
48 Mitragotri, S. Role of Nanoparticle Size, Shape and
49 Surface Chemistry in Oral Drug Delivery. *J. Control.*
50 *Release* **238**, 176 (2016).
- 51 194. Panariti, A., Miserocchi, G. & Rivolta, I. The effect
52 of nanoparticle uptake on cellular behavior:
53 disrupting or enabling functions? *Nanotechnol. Sci.*
54 *Appl.* **5**, 87 (2012).
- 55 195. Zhu, M. *et al.* Physicochemical properties determine
56 nanomaterial cellular uptake, transport, and fate. *Acc.*
57 *Chem. Res.* **46**, 622–631 (2013).
- 58 196. Agrawal, P. *et al.* CPPsite 2.0: a repository of
59 experimentally validated cell-penetrating peptides.
60 *Nucleic Acids Res.* **44**, D1098–D1103 (2016).
197. Favaro, M. T. de P. *et al.* Switching cell penetrating
and CXCR4-binding activities of nanoscale-
organized arginine-rich peptides. *Nanomedicine*
Nanotechnology, Biol. Med. **14**, 1777–1786 (2018).
198. Nakase, I. *et al.* Arginine-rich cell-penetrating
peptide-modified extracellular vesicles for active
macropinocytosis induction and efficient intracellular
delivery. *Sci. Reports 2017 71* **7**, 1–11 (2017).
199. Cho, C. F. *et al.* Blood-brain-barrier spheroids as an
in vitro screening platform for brain-penetrating
agents. *Nat. Commun. 2017 81* **8**, 1–14 (2017).
200. Sharma, G., Lakkadwala, S., Modgil, A. & Singh, J.
The Role of Cell-Penetrating Peptide and Transferrin
on Enhanced Delivery of Drug to Brain. *Int. J. Mol.*
Sci. **2016, Vol. 17, Page 806** **17**, 806 (2016).
201. Ahlschwede, K. M. *et al.* Cationic carrier peptide
enhances cerebrovascular targeting of nanoparticles
in Alzheimer's disease brain. *Nanomedicine*
Nanotechnology, Biol. Med. **16**, 258–266 (2019).
202. Eshraghi, A. A. *et al.* Preclinical and clinical
otoprotective applications of cell-penetrating peptide
D-JNKI-1 (AM-111). *Hear. Res.* **368**, 86–91 (2018).
203. Kristensen, M. *et al.* Penetratin-Mediated
Transepithelial Insulin Permeation: Importance of
Cationic Residues and pH for Complexation and
Permeation. *AAPS J.* **17**, 1200–1209 (2015).
204. Guo, F. *et al.* Enhanced oral absorption of insulin
using colon-specific nanoparticles co-modified with
amphiphilic chitosan derivatives and cell-penetrating
peptides. *Biomater. Sci.* **7**, 1493–1506 (2019).
205. Yang, Y. *et al.* Cell-penetrating peptide-modified
quantum dots as a ratiometric nanobiosensor for the
simultaneous sensing and imaging of lysosomes and
extracellular pH. *Chem. Commun.* **56**, 145–148
(2019).
206. Guo, P. *et al.* Nanoparticle elasticity directs tumor
uptake. *Nat. Commun.* **9**, 130 (2018).
207. Anselmo, A. C. *et al.* Elasticity of Nanoparticles
Influences Their Blood Circulation, Phagocytosis,
Endocytosis, and Targeting. *ACS Nano* **9**, 3169–3177
(2015).
208. Pei, D. & Buyanova, M. Overcoming Endosomal
Entrapment in Drug Delivery. *Bioconjug. Chem.* **30**,
273 (2019).
209. Bus, T., Traeger, A. & Schubert, U. S. The great
escape: how cationic polyplexes overcome the
endosomal barrier. *J. Mater. Chem. B* **6**, 6904–6918
(2018).
210. Stanzl, E. G., Trantow, B. M., Vargas, J. R. &
Wender, P. A. Fifteen years of cell-penetrating,
guanidinium-rich molecular transporters: basic
science, research tools, and clinical applications. *Acc.*
Chem. Res. **46**, 2944–2954 (2013).
211. Dalal, C. & Jana, N. R. Multivalency Effect of TAT-
Peptide-Functionalized Nanoparticle in Cellular
Endocytosis and Subcellular Trafficking. *J. Phys.*
Chem. B **121**, 2942–2951 (2017).
212. Guo, X. *et al.* Multifunctional nanoplateforms for

- 1
2
3 subcellular delivery of drugs in cancer therapy. *Prog.*
4 *Mater. Sci.* **107**, 100599 (2020).
- 5 213. Xu, X. *et al.* Ultra-pH-Responsive and Tumor-
6 Penetrating Nanoplatfrom for Targeted siRNA
7 Delivery with Robust Anti-Cancer Efficacy. *Angew.*
8 *Chemie Int. Ed.* **55**, 7091–7094 (2016).
- 9 214. Parodi, A. *et al.* Enabling cytoplasmic delivery and
10 organelle targeting by surface modification of
11 nanocarriers. *Nanomedicine* **10**, 1923 (2015).
- 12 215. Biswas, S., Dodwadkar, N. S., Deshpande, P. P. &
13 Torchilin, V. P. Liposomes Loaded with Paclitaxel
14 and Modified with Novel Triphenylphosphonium-
15 PEG-PE Conjugate Possess Low Toxicity, Target
16 Mitochondria and Demonstrate Enhanced Antitumor
17 Effects In Vitro and In Vivo. *J. Control. Release* **159**,
18 393 (2012).
- 19 216. Chen, C., Turnbull, D. M. & Reeve, A. K.
20 Mitochondrial Dysfunction in Parkinson’s Disease—
21 Cause or Consequence? *Biology (Basel)*. **8**, (2019).
- 22 217. Klein, K. *et al.* Role of Mitochondria in Cancer
23 Immune Evasion and Potential Therapeutic
24 Approaches. *Front. Immunol.* **11**, 2622 (2020).
- 25 218. Kim, S., Nam, H. Y., Lee, J. & Seo, J.
26 Mitochondrion-Targeting Peptides and
27 Peptidomimetics: Recent Progress and Design
28 Principles. *Biochemistry* **59**, 270–284 (2019).
- 29 219. Klimpel, A. & Neundorf, I. Bifunctional peptide
30 hybrids targeting the matrix of mitochondria. *J.*
31 *Control. Release* **291**, 147–156 (2018).
- 32
33
34
35
36
37
38
39
40
41
42
43
44
45
46
47
48
49
50
51
52
53
54
55
56
57
58
59
60